NASA Contractor Report 185208

Instantaneously Generated Foam and Its Applicability to Reduced Gravity

Ali Ilhan, Dong-Sang Kim, and Pavel Hrma
Case Western Reserve University
Cleveland, Ohio

February 1990

Prepared for
Lewis Research Center
Under Grant NAG3-740

National Aeronautics and
Space Administration

CONTENTS

1. SUMMARY

The objective of this study is two-fold : (i) understanding the generation and collapse of foam in molten glass and (ii) determining the role of gravity in transient foam dynamics. Both theoretical considerations and experiments show that gravity affects evolution of transient foams. Provided that Marangoni forces are absent, the lack of bubble motion under microgravity will prevent formation of surface foam and, as a result, only bulk foam will be generated. Also, the absence of gravity drainage will affect the foam collapse rate and mode when a surface foam has been produced prior to its exposure to microgravity.

The progress of this work follows three steps: (i) selection of appropriate materials and development of experimental techniques, (ii) experimental study of transient foams on earth and developing a theoretical model, and (iii) experimental study of transient foams under microgravity during free fall in a drop tower. This report presents the main results of the first phase of the research which involves most of the ground based work needed to accomplish the first two steps. The suggestions for the final stage of the work is also included.

Earth bound experiments have shown that it is possible to produce transient foams suitable for drop tower experiments and to record their behavior by a video or still camera in a simple experimental set-up. Transient cellular foams were produced and studied in soda lime glass with sulfate at 1400-1500°C. The study of foams in model systems under convenient ambient temperature conditions helped to gather a significant amount of information in a short time. The relationship between foam behavior and structure has been analyzed and the relationship between foam structure and the system properties is currently under development.

2. INTRODUCTION

Foam behavior is governed by eight independent forces (Table 1). Four of these forces (electrostatic, steric, van der Waals, and Marongoni) control the behavior of persistent foams, but are not significant for transient foams. The four remaining forces are the viscous drag, internal pressure, gravity, and capillary forces. Among these forces, the viscous drag and pressure force can be controlled by experimental conditions, such as temperature, external pressure, or degree of oversaturation by a foaming agent. Two forces, the capillary force and gravity force, can be effectively separated only by reduced gravity. This study is confined to transient foams because these foams are more sensitive to gravity than persistent foams. Transient foams frequently occur in molten glasses [1-10] and are also common in metallurgy [11,12], petrochemistry [13,14], and the food industry [15,16].

Glass was chosen as a foaming medium because some fundamental problems regarding glass foams, such as the existence of surface active agents in molten glasses or bubble nucleation on solid particles, can be addressed in the course of the research. In addition, molten glass is advantageous to microgravity applications, in that a gas phase can be generated within the melt uniformly by a chemical reaction. The uniformity of nucleation is assured if the bubbles nucleate on residual refractory grains from the glass batch and if these grains are uniformly distributed in space. Also, the rate of gas phase generation and melt viscosity can be controlled in a range wider than in any other medium which provides wider range of experimental conditions. The high viscosity of molten glass requires either a relatively long experimental time or a sensitive experimental technique to record changes produced by gravity and capillary forces within a short time.

Significant information can be learned via the study of foams in model systems under convenient ambient temperature conditions. Since viscosity of aqueous liquids is very low, application of mild surfactants is necessary to make their lifetime comparable with the free fall time

in the drop tower. Both systems, molten glasses and aqueous liquids were used in our study and are being considered for microgravity experiments.

The criterion for selecting a glass system for foam study is the ability of the glass to produce gravity sensitive foam with a low volatilization rate. Since soda-lime glass with sodium sulfate as a foaming agent satisfies these requirements better than other systems tested [17], it was chosen for further investigation. Earlier discussions of our experiments at NASA Lewis led to the investigation of the possibility of replacing sulfate, which produces foam above 1400°C, with a gas liberating agent at lower temperatures. This would also require changing the composition of the basic glass. Attempts to identify such systems were unsuccessful. However, it later appeared that $T \geq 1400°C$ can be used with an equipment modification.

A reproducible method should generate almost identical foam structure if identical conditions are maintained and should be suitable for experiments in a microgravity environment. A widely used method, such as mechanical shaking does not reproduce identical foam structure. Monsalve and Schechter [18] report that foams generated by shaking did not collapse in a reproducible manner. Another established method, bubbling, can be applied only prior to application of microgravity. Moreover, according to Watkins [19], foam height produced by bubbling a gas through viscous oils in cylindrical containers varies in a wide range when experiments are repeated under presumably identical conditions. Also, neither shaking nor bubbling can be conveniently applied to molten glass. First attempts, consisting of the generation of foam by mechanical agitation, such as pouring and shaking of an aqueous liquid oversaturated with a gas, were discontinued due to the difficulty in controlling initial parameters and will not be included in this report.

The lack of satisfactory foam generation methods goes hand in hand with lack of theoretical understanding. Although the behavior of persistent foams is well understood [20-22], the models for transient foams are limited to steady state [23-25]. This lack of established methods for reproducible generation and collapse of foams and lack of an adequate theoretical model for non-

steady transient foams were two obstacles that had to be overcome before microgravity can be successfully applied to the investigation of transient foams. Both obstacles have been resolved by our previous efforts. A theoretical model for non-steady generation and collapse of transient foams is outlined in the Theoretical section. This theory has been developed in this work. Two reproducible foam generation methods based on gas liberation from an oversaturated liquid are described in the Experimental section.

Both methods are based on liberation of gas from oversaturated liquids. Here only the basic ideas of these methods will be mentioned. Since gas bubbles are nucleated within the liquid, no introduction of gas phase from outside is required. In glasses prepared from batches, heterogeneous interface for bubble nucleation is provided by residual silica grains. Oversaturation can be achieved either by increasing temperature above the equilibrium temperature or reducing pressure below the equilibrium pressure [3,5,6,26,27]. To control bubble nucleation in aqueous liquids, a granular solid was added. Oversaturation was produced by pressure decrease.

The foam generation methods differ in the sequence of the nucleation agent addition and pressure decrease. In the reduced pressure method, the nucleation agent is placed into the liquid before the pressure is reduced; in the nucleation agent addition method, pressure is reduced before the nucleation agent is added and foam is generated by dropping the nucleation agent in the gas oversaturated liquid. Both methods were applied to aqueous liquids oversaturated with carbon dioxide which were placed in hydrophobic containers to prevent bubble nucleation on container walls. A summary of different foam generation methods is shown in Table 2a and b. The pertinent features of both high and low temperature systems are summarized in Table 3.

Foam height vs. time data were extracted from the video-still images and later evaluated to determine the collapse coefficient. Influential parameters, including nucleation particle characteristics (type, amount, size, shape, and roughness), coating agent (type, quality, and its application procedure), and injection technique (dropping height, and angle) were optimized. To

identify the optimum parameters, a large number of experiments were needed which could not be effectively performed at high temperatures. Therefore, a room temperature model liquid was used.

The work including both molten glasses and aqueous liquids evolves in the following three stages:

1. Selection of appropriate materials and development of experimental techniques.
2. Experimental study of transient foams on earth and developing a theoretical model.
3. Experimental study of transient foams under microgravity during free fall in a drop tower.

Most of the ground-based work related to the first two points above was accomplished under the first phase of this research (Phase 1; NASA Grant NAG 3-740). The third point is the subject of the proposal submitted in June 89 (Phase 2).

3. THEORY

The relationship between the acting forces and foam behavior involves two steps: the connection between foam structure and foam behavior, and the link between the material and environmental parameters and foam structure.

3.1. Relation between Foam Structure and Behavior

Gas phase volume, V, within the liquid is subjected to the gas balance equation

$$dV/dt = r_I + r_G - r_R \qquad \text{Eq. 1}$$

where r_I is the rate of gas injection from outside, r_G the rate of gas phase generation within the liquid, and r_R the rate of gas release from the liquid to the environment. Introducing the relative gas phase volume

$$\varepsilon = V / V_T \qquad \text{Eq. 2}$$

where V_T is the total gas phase volume generated and injected, and integrating Eq. 1, we obtain

$$\varepsilon = \varepsilon_I + \varepsilon_G - \varepsilon_R \qquad \text{Eq. 3}$$

where $\varepsilon_I = V_T^{-1} \int_0^t r_I \, dt$, $\varepsilon_G = V_T^{-1} \int_0^t r_G \, dt$, and $\varepsilon_R = V_T^{-1} \int_0^t r_R \, dt$.

We shall restrict our attention to the process in which there is no gas injection, i.e., $r_I = 0$, and gas generation can be described by the exponential function

$$\varepsilon_G = 1 - \exp(- K_G t) \qquad \text{Eq. 4}$$

where K_G is the gas phase generation rate coefficient.

The gas release rate can be expressed as

$$r_R = k \, r_s \, A / t_s \qquad \text{Eq. 5}$$

Where r_s is the effective top bubble radius, A is the foam surface area, and t_s is the residence time of a top bubble. If $r_I = 0$ and $r_G = 0$, then, by Eq. 5, Eq. 1 reduces to $dV/dt = 2 \, r_s \, A / t_s$. The factor k is close to 2 for simple foam cell geometries. The residence time and the effective top bubble radius are generally functions of the relative gas phase volume and time. Let us assume that they are simple power-law functions of ε:

$$r_s = r_{so} \, \varepsilon^b \qquad t_s = t_{so} \, \varepsilon^c \qquad \text{Eq. 6}$$

where t_{so} is the initial residence time of a top bubble, r_{so} is the initial effective top bubble radius, and b and c are constants. By Eq. 5 and 6

$$\varepsilon_R = K_R \int_0^t \varepsilon^{1-n} \, dt \qquad \text{Eq. 7}$$

where $K_R = 2\, r_{so} A / V_T\, t_{so}$ is the gas phase release rate coefficient and $n = 1 - b + c$ is the gas release susceptibility. Let three special cases be mentioned:

For n = 0 (exponential release), Eq.'s 3, 4 and 7 yield

$$\varepsilon = (K_R / K_G - 1)^{-1} [\exp(- K_G t) - \exp(- K_R t)] \qquad \text{Eq. 8}$$

for n = 1 (linear release)

$$\varepsilon = 1 - \exp(- K_G t) - K_R t \qquad \text{Eq. 9}$$

for $K_G \rightarrow \infty$ (instantaneous generation)

$$\varepsilon = (1 - n\, K_R\, t)^{1/n} \qquad \text{Eq. 10}$$

The right side of Eq. 8 is a difference of two exponentials. Foam height decreases gradually as time progresses. This behavior is typical for a foam in which smaller and smaller cells take longer and longer time to collapse. Such a foam may result from bubble separation when they ascend to the liquid surface. A foam consisting of equally sized cells, which break after equal residence times, will fit in the category represented by Eq. 9. Eq. 10 allows us to see the effect of n. Generally, the collapse susceptibility can assume values between minus infinity and plus infinity, covering a wide range of foam behavior (Table 4). As Fig. 1 reveals, only non-positive values of n represent transient foams.

The linear release model closely approximates the behavior of foams in molten glasses as well as in aqueous liquids. The foam lifetime, t_L, (the time at which $\varepsilon = 0$) and the maximum relative gas phase volume, ε_M, are given by the equations

$$K_R t_L = 1 - \exp(- K_G t_L) \qquad \text{Eq. 11}$$

and

$$\varepsilon_M = 1 - [1 + \ln(K_G / K_R)] K_R / K_G \qquad \text{Eq. 12}$$

Since the $\varepsilon(t)$ curve is determined by two coefficients, K_G and K_R, it can be represented by a point on (K_G, K_R) plane. Fig. 2 shows lines of constant foam lifetime and maximum relative gas phase volume on this plane together with the regions of aqueous and soda-lime glass foams.

3.2. Relation between Foam Structure and Properties

Foam properties and conditions under which foam evolves are manifested by four forces: pressure force, viscous drag, capillary force, and gravity (Table 1).

1. Pressure Forces Bubble generation and growth in a gas oversaturated liquid is produced by the difference between partial pressure of the gas in the liquid and the overall pressure (Fig. 3a). Undesirable expansion or shrinkage of cells can result from fluctuations of the pressure above the foam and should be avoided. Pressure forces may cause cell expansion and cell wall burst if the cell gas and cell wall liquid are not at equilibrium. However, if the walls separating the cells are sufficiently thin, chemical and phase equilibrium within the foam will be established quickly.

2. Viscous drag opposes gravity, capillary, and pressure forces. Strong pressure forces must be applied to overcome viscous drag in high viscosity liquids if the foam generation time is limited. The resulting tendency toward bulk foam generation [25] makes such foams less sensitive to gravity. For more details see Appendix I. Glass melts for short time microgravity experiments must have viscosity lower than 10 Pas.

3. Capillary Forces produce cell wall drainage by suction of liquid from cell walls to Plateau borders (Fig. 3b). These forces do not act in spherical foams. Another action of capillary forces is prominent in persistent foams and consists of stabilizing critically thin lamellae by Gibbs and Marangoni effects [28].

4. Gravity plays a crucial role in foam formation on the free surface of a liquid. Under zero gravity, only bulk foam can be produced if bubble nucleation within the liquid is sufficiently uniform. Foam drainage by gravity (Fig. 3c) converts spherical foam to cellular foam and causes cell wall thinning to critical thickness. In the absence of both gravity and pressure forces, capillary forces alone will determine foam behavior: (i) spherical foams will not be affected, (ii) "wet" cellular foams ($2r_f > s$, see Appendix II) will tend to spheroidize, and (iii) "dry" cellular foams ($2r_f \leq s$, see Appendix II) will tend to collapse.

Two hydrodynamic models are available for transient foams in which pressure forces are absent. Hartland and Barber [23] analyzed capillary suction and gravity drainage of transient cellular foams. Leonard and Lemlich [24] considered the effect of surface viscosity but did not include capillary forces. Both models are restricted to a steady state. In Hartland and Barber's model [23], the steady state is established as a result of a balance between the influx of gas to the surface foam from below and gas release by top bubble breakage. Leonard and Lemlich [24] consider foam overflow and continuous supply of fresh liquid. The limits of the steady state and its breakdown was analyzed by Hrma [25]. More work will be required to adopt these models to the transient situation when foam expands and collapses within a finite time.

4. EXPERIMENTAL PROCEDURES AND MATERIALS

4.1. Molten Glass

The Phase 1 experiments with molten glasses were conducted in a special furnace [29]. The furnace has the following features (Fig. 4) : (i) a transparent quartz crucible allows visual observation of foam; (ii) dark background behind the crucible yields improved contrast for photography; and (iii) pressure can be reduced in the crucible instead of the entire furnace interior.

To generate foam, a mixture of silica sand, sodium carbonate, calcium carbonate, and foaming agent (sodium sulfate) was heated to the foaming temperature, at which the batch was converted to melt with residual silica sand. Isothermal treatment (samples placed into a pre-heated furnace) was used for the measurement of kinetic coefficients. Ramp heating (14 °C/min.) to the set temperature was used for determination of foam starting temperature. The residual solid particles provided sites for bubble nucleation. The composition of soda-lime glass was 74 SiO_2, 16 Na_2O, and 10 CaO in weight percent with sulfate (corresponding to 1% SO_3) as the foaming agents.

4.2. Room Temperature Liquids

The experimental set-ups for the pressure decrease method, and the nucleation agent addition method are shown in Fig.'s 5 and 6. The transparent containers were 7 cm high and had a 2.9 cm diameter. The nucleation agent for the pressure decrease method was 0.5 g of silica with particle size 124-248 μm. The dropping technique for the nucleation agent addition method was improved and modified in the course of the experiments. Initially, it consisted of dumping the particles into the liquid. Later, using a funnel with various nozzle sizes and different potential heads over the liquid improved the consistency of the results.

As an aqueous liquid oversaturated with carbon dioxide, a carbonated soft drink (Coca Cola™) was used from commercially available cans (16 oz.). Because of possible variability of this material, for each reproducibility experiment set, the liquid was taken from the same can and the experiments were carried out immediately one after another. The liquid was carefully transferred to the container to avoid premature bubbling.

Three commercially available coating agents for containers were used. Two were oil-based, 711™ and TriFlow™ with teflon, and one was alcohol-based, Rain-X. The coating procedure involved cleaning the containers with Micro™ (laboratory ultrasonic cleaning liquid) in

an ultrasonic cleaner for 1 h, washing with distilled water, drying in air for 24 h, coating, and drying in air for 24 h.

Recording equipment consisted of a digital video camera with a built-in stopwatch, VCR, still frame photography device, TV monitor, and fiber optic light source. A 135 mm SLR lens and macro extension tube were attached to the video camera. Three fiber optic light source devices in conjunction with a light diffuser gave adequate front and back lighting conditions for best results. Experiments were recorded at 30 frames per second. Foam height was measured from still images preferably at 0.5 second intervals.

Foam height measurement is shown in Fig. 7. For the pressure decrease method and some experiments involving addition method, the foam height, H_F was measured and plotted against time. For a large portion of the addition experiments (A31 and later, Table 7), the total height, H_B,was used because the interface between the liquid and foam was too difficult to determine.

5. RESULTS

5.1. Molten Glass

Generation and collapse of foam in soda-lime glass was studied by Kim and Hrma and the details will be published elsewhere [29-31]. Here only results pertinent for this microgravity work will be summarized.

The effect of the melting temperature and the initial silica grain size on the maximum foam height for batches which contained 4% of total Na_2O from Na_2SO_4 (1% SO_3 in glass) and is shown in Fig. 8. The batches were isothermally heated under atmospheric pressure. The effect of the initial sulfate concentration on the maximum foam height and foam starting temperature for coarse silica batches ramp heated at 14°C/min. is given in Fig. 9. The initial foam generation rate and the foam collapse rate, evaluated graphically, are plotted in Fig. 10 for isothermal heat

treatment. Fig. 10 shows that the collapse rate is affected by the silica grain size and temperature. An example of gas phase holdup vs. time dependence is plotted in Fig. 11, in which the experimental data were fitted by Eq. 9. The values of parameters for 1475°C are $K_G = 1.7 \times 10^{-2}$ s^{-1}, and $K_R = 2.6 \times 10^{-3}$ s^{-1}. By Eq. 11 and 12, $t_L = 400$ s, and $\varepsilon_M = 0.6$. The average top bubble radius was $r_B = 2$ mm.

Assuming that the size of the bubbles at the top surface is constant, the top surface bubble residence time was calculated by Eq. 5. The residence time and number of bursts of top surface bubbles are shown in Table 5 for different temperatures.

In summary, sulfate foam generation is controlled by sulfate oversaturation and surface area for bubble nucleation. The sulfate oversaturation is determined by the initial sulfate concentration and melting temperature and the surface area for bubble nucleation is determined by the initial silica grain size and thermal history of the batch. Hence, the parameters controlling foam generation are the initial content of foaming agent, the foaming temperature (sulfate oversaturation), the rate of heating to the foaming temperature (thermal history), and the initial size of silica grains (nucleation area).

5.2. Room Temperature Liquids

5.2.1 Pressure Decrease Method

Experiments were initially conducted in uncoated containers without nucleation agent. The final pressure varied from 10 to 30 kPa. The foam height increased as the final pressure decreased (Fig. 12). Pressures lower than 20 kPa resulted in satisfactory foam height (> 10 mm). Reproducibility was poor and the size distribution of the foam cells was wide. With an addition of silica particles and container coating, lower pressure decrease was needed to generate foam of a given height (24 kPa as compared to 17 kPa without silica) and bubbles were more uniform in size. When an oversaturated liquid in a coated container without nucleation agent was exposed to a sudden pressure decrease to 13 kPa, no bubbles were formed.

Even with coated containers and nucleation agent, reproducibility was less than satisfactory. After ~ 1 second, cells started coarsening through coalescence, especially at the upper layer of the foam. This coarsening, probably the source of poor reproducibility, is caused by pressure fluctuations which will be avoided with a better pressure stabilizing equipment.

Pressure decrease generated foam within ~ 1-2 seconds. Collapse of the foam took 4-5 seconds on the average. The total lifetime of the foam was ~6 seconds. The average bubble size was 1 mm in diameter. Bubble counts and size measurements taken at different constant depths with regards to the top surface with time indicated that most of the coalescence occurred within ~3 mm below the top surface. The measured survival time of top surface bubbles was 0.1-0.2 seconds for foam in a pressure decrease experiment. This agrees well with the value calculated by Eq. 5 for 1 mm bubble diameter.

5.2.2. Nucleation Agent Addition Method

A total of 83 experiments was performed with the nucleation agent addition method to optimize the experimental variables, the most important of which are summarized in Table 6. These variables fall into three categories: (i) nucleation agent variables: the material, quantity, particle size, shape, distribution, and surface roughness, (ii) coating agent variables: the material, and coating and drying procedure, (iii) dropping technique variables: the dropping angle, and height over the liquid. A summary of results listed in Table 7.

5.2.2.1. Nucleation

Both soluble and insoluble particles were used. The idea of using soluble agents, sugar ($C_{12}H_{22}O_{11}$) and salt (NaCl), was to simulate the behavior of silica grains in glass melts. However, the soluble agents remained nearly undissolved during the experimental time of ~10 seconds, whereas the residual silica entirely dissolves during foaming of sulfate in soda-lime glasses.

Maximum height vs. addition mass for sugar is plotted in Fig. 13 showing that as the addition mass increases, more foaming takes place. Later trials with alumina revealed a similar behavior. More foaming with increasing nucleation agent mass was expected because more bubbles can be nucleated from larger surface. This would increase the foam generation rate. Surprisingly, the time corresponding to maximum height also increases with increasing mass (Fig. 14). The reason might be that, since the time recording was started when the first particle entered the liquid, for increased mass more time elapsed until the addition was complete.

Alumina, silica particles, granulated brick, glass beads, and metallic balls were employed as insoluble agents. When the addition mass of alumina particles was held constant (= 0.1 g) with particle sizes varied, very fine alumina particles, 0.3 μm, produced almost no foam. The reason was that the fine particles floated on the liquid surface for some time after dropping and sank into the liquid gradually as time progressed. Heavier particles penetrated the liquid quickly but with larger particle size the nucleation surface decreased. Grain size of 600-840 μm was optimum for alumina. Large (5 mm) and heavy metallic balls caused extensive mechanical turbulence in the liquid.

Ceramic particles (alumina) with rough surfaces generated more bubbles than smoother silica particles of comparable size and, as a result, promoted more foaming. Granular brick (600-841 μm) (mass=0.5 g) with a very rough surface was too light and floated. Glass beads and metallic balls with smooth surfaces resulted in lower foam height and a longer lifetime.

5.2.2.2. Coating

Coating reduced standard deviation of the collapse coefficients, both linear and exponential, to one half of that for uncoated containers (Table 8). Triflow™ was the least effective. 711™ was the best. However, the surface coated by agent 711™ appeared wet even after 192 h of drying at 150°C. In contrast, surfaces treated by Rain-X™ appeared dry. Rain-X was used with glass beads and metallic balls. One coating layer was sufficient for all agents.

5.2.2.3. Dropping

Experiments with different nozzle diameters showed that the nozzle should be narrow enough to direct the particles to the middle of the container but large enough to prevent possible clogging. The optimum nozzle diameter was dependent on the particle size and varied from 4 to 15 mm. If the dropping height above the liquid was too short, wetting of the nozzle by the foaming liquid caused clogging. If it was too large, mechanical agitation and gas entrapment interfered with nucleation. The optimum dropping height was dependent on the particle size and density and varied from 5.5 to 8 cm.

5.2.2.4. Data Evaluation and Results

A characteristic result of foam height vs. time data with three different nucleation agents is shown in Fig. 15. The linear and exponential coefficients were evaluated as a slope of the foam height and the logarithm of the foam height vs. time. The exponential collapse coefficient, K_{cc}, and the intercept, I_{ec} were determined by taking the natural logarithm of height vs. time curves and fitting a line to the linear portion of the collapse segment. The linear collapse coefficient, K_{lc}, and intercept, I_{lc} were determined by taking the height vs. time curves and fitting a line to the linear portion of the collapse curve. The steps are schematically indicated in Fig. 16 for experiment with alumina particles as a nucleation agent.

The findings and the experimental conditions are summarized in Table 7. The height range is shown as the difference between maximum and minimum height. Maximum height includes the height increase due to addition of solid particles and due to gas build-up. Minimum height is the remaining height after the foam collapses. The average values of the experiments for each set are shown in Table 8.

The fitting of Eq. 8 & 9 to the experimental data was performed for selected data. Linear evaluation fitted the data better than exponential evaluation. An example of a linear collapse is

shown in Fig. 17. Foam collapse was close to linear especially with metallic balls and glass beads as nucleation agents. A non-linear collapse (Fig. 18) occurred in some trials with alumina particles. A reasonably good reproducibility was achieved as shown in Fig. 15. The foam collapse rate exhibits a better reproducibility than the maximum foam height.

Foam was generated in ~2-3 s, the collapse time was ~6-15 seconds, and the total lifetime was ~8-18 seconds. Typical values for aqueous liquids are gas generation rate constant (K_G) = 0.725 s^{-1}, gas release rate constant (K_R) = 0.069 s^{-1}, total lifetime (t_L) = 15 s, and maximum relative gas phase holdup (ε_M) = 0.7. The average bubble size was ~0.1 mm in diameter, ~10 times smaller than the foam cells obtained by the pressure decrease method. Several larger bubbles (~1 mm in diameter) were scattered within the foam especially in the vicinity of the top surface. The average diameter of all bubbles at the top surface was close to 1 mm or larger.

A comparison of foams generated by pressure decrease and nucleation agent addition methods is shown in Table 9. Despite the difference in cell size, the collapse rate was similar, 4-6 mm/s for pressure decrease and ~2-5 mm/s for nucleation agent addition. This is due to the similar size of top surface bubbles. The substantial increase in bubble size on reaching the top surface in foam generated by nucleation agent addition was a result of massive coalescence.

6. DISCUSSION

The total collapse time of sulfate foams in molten soda-lime glass is approximately 400 seconds. Although only a short portion of the foam lifetime is required for microgravity exposure, the lifetime of soda-lime glass foam may be shortened if glass with higher alkali and alkaline earth content is used. This is currently being tested. However, even with the present glass composition, five second free fall in a drop tower is sufficient to determine the change in the foam collapse rate. The average bubble diameter determined from a photograph is 4 mm. With the foam collapse rate of 0.1 mm/s and the foam surface area of 400 mm^2, this corresponds to an average

bubble residence time at the top surface of 0.9 to 4 s and 30 to 135 bursts of a bubble within five seconds as indicated in Table 5. The number of bursts will be increased when a glass with lower viscosity and a larger foam surface area is used. Additional information about microgravity effects will be produced by measurement of the thinning rate of the lamellae.

Glass and aqueous foams are similar: foams form exponentially and collapse in a linear fashion (Fig. 11 vs. Fig. 17). Consequently, both foams can be represented by Eq. 9. This similarity between high and low temperature transient foams allows a simple room temperature modelling of glass foam inspite of the big difference in kinetic properties of both systems. The lifetimes along with maximum relative gas phase volume for glass and aqueous foams are mapped in Fig. 2. The darker lines represent available microgravity experimental time.

7. REDUCED GRAVITY APPLICATION

Reduced gravity will be employed at the Zero-Gravity Research Facility at NASA Lewis Research Center. The facility consists of a 145 m evacuated drop tower, which is 6.1 m in diameter and can be evacuated to 10^{-2} torr. This level of vacuum reduces the aerodynamic drag on the package to less than 10^{-5} g. Five seconds of low gravity can be obtained on a standard drop. Ten seconds of low gravity can be obtained by accelerating an experimental package up from the bottom followed by free fall back down to the deceleration tank at the bottom. However, it is anticipated that the facility will be operated almost exclusively in the five second drop mode. In addition, high acceleration, to which the experimental package is exposed prior to the ten seconds of low gravity, would disturb liquid in containers and may affect the equipment. Therefore, the experiment time for low gravity is limited to five seconds.

For room temperature liquids, two experimental arrangements are considered. A simple design for the nucleation agent addition method adapted to the drop tower is shown in Fig. 19. The arrangement includes a synchronized particle release mechanism. This set-up includes a

battery of five rectangular 2 x 1.5 cm containers. The release mechanism will drop the nucleation agent either simultaneously or at one second intervals to expose foams at different stages of evolution to microgravity or to compare the reproducibility of a particular experiment during a single drop of the package.

A similar arrangement for the pressure decrease method (Fig. 20) will consist of a container, pressure gauge, and a solenoid valve. The container will be connected to a low pressure vessel, in which a constant pressure will be maintained by a pressure sensor operated valve. For a multiple experiment set-up, a battery of five rectangular 2 x 1.5 cm containers will be decompressed either simultaneously or in one second intervals, so that the foams at different stages of evolution are exposed to microgravity during a single drop of the package. It is important that pressure is constant after decompression to avoid undesirable contraction or expansion of foam cells.

For experiments with soda-lime glass, a modified version of the furnace used for the earth based experiments will be constructed. Melting will start from the batch containing sodium carbonate, calcium carbonate, silica sand, and sodium sulfate. A battery of two or three transparent quartz crucibles of rectangular cross-section, 6 x 20 mm, and 150 mm height, will be inserted into the furnace through the top opening. This arrangement will permit the upper part of the crucibles to be maintained at ambient temperature and will allow control of the pressure individually in each crucible. The furnace will be operated at constant temperatures up to 1600°C. A quartz front window and dark background (a closed ceramic tube with a cool end) will facilitate recording by a high speed camera. Each crucible will be equipped with a Pt-Rh thermocouple and a solenoidal valve to apply pressure jumps in the prescribed time intervals if required. The valve will connect the crucibles with a low pressure vessel, in which a constant pressure will be maintained by a pressure sensor operated valve.

Crucibles with glass batch samples will be placed into the furnace preheated at the temperature about 50°C above the set temperature. Foaming temperatures will be in the range of

1350 to 1500°C. Pressure and time to trigger foaming will depend on the temperature and silica grain size (some undissolved silica residues are needed for bubble nucleation). Valves will be open either simultaneously or in 30-60 second time intervals to observe different stages of collapse in one experiment. Alternatively, identical conditions will allow to increase the effective surface area.

For microgravity application, it is our intention to prepare a laboratory room temperature transient foam with well defined and controlled properties, and to improve the design of the pressure decrease equipment for room temperature foams. Also, it is desirable to reduce glass melt viscosity at foaming temperatures by modifying glass composition and to investigate the possibility of a more rapid collapse of glass foams using arsenic instead of sulfate.

8. CONCLUSIONS

Soda-lime glass with sulfate as foaming agent was found suitable for study of glass foams. An aqueous liquid oversaturated with CO_2 is an adequate room temperature foaming model although the kinetic properties of room temperature liquids and molten glass are different.

Novel experimental methods for study of foaming in glass and room temperature liquids were developed. A custom-designed furnace enables direct observation of the foam at 1350-1500°C. Pressure decrease and nucleation agent addition methods were developed to produce foams in a room temperature model fluids. Experiments have shown that it is possible to produce glass and room temperature foams in a reproducible manner.

The lifetime of glass foam is approximately 400 seconds. The number of cell-burst events during 5 seconds of microgravity time is sufficient to determine the effect of microgravity. The lifetime of aqueous foams is about 15 seconds. Hence, with both foams it is feasible to determine the effect of reduced gravity in a drop tower.

A theoretical model for generation and collapse of transient foams was applied to the experimental data showing that both foams exhibit the same type of behavior, namely, exponential gas phase generation and linear gas phase release. This behavior can be represented by two kinetic coefficients. The gas phase release coefficient is related to the cell size and residence time.

9. LITERATURE

1. Emer, P., "Foam formation in glass melting tanks," Glastech. Ber., **42**, 221-28 (1969) in German.

2. Pieper, H., "Batch charging in all-electrical tanks,"Glastech. Ber., **52**, 229-36 (1979) in German.

3. Gerrard, A. H., and Smith, I. H., "Laboratory techniques for studying foam formation and stability in glass melting," Glastech. Ber., **56K**, Vol.1, 13-8 (1983).

4. Waldecker, G. G., "Foam in glass melting," Glastek. Tidskr., **38**, 3-7 (1983) in Swedish.

5. Goldman, D. S., Brite, D. W., and Richey, W. C., "Investigation of foaming in liquid-fed melting of simulated nuclear waste glass," J. Amer. Ceram. Soc., **69**, 413-17 (1986).

6. Goldman, D. S., "Melt foaming, foam stability and redox in nuclear waste vitrification," J. Non-Cryst. Solids, **84**, 292-98 (1986).

7. Bickford, D. F., Hrma, P., Bowen, B. W., and Smith, P. K., "Control of radioactive waste-glass melters," Amer. Ceram. Soc. Bull., to be published.

8. Ahn, J. S., and Hrma, P., "The effect of heat treatment on foaming of simulated nuclear waste in a borosilicate glass melt," Nuclear Waste Management II, **20**, p.181-90, American Ceramic Society, Westerville, Ohio, 1986.

9. Lucktong, C., and Hrma, P., "Oxygen evolution during MnO - Mn_3O_4 dissolution in a borosilicate melt," J. Amer. Ceram. Soc., **71**, 323-28 (1988).

10. Kappel, J., Conradt, R., and Scholze, H., "Foaming behavior on glass melts," Glastech. Ber., **60**, 189-201 (1987).

11. Kozakevitch, P., "Foams and emulsions in steelmaking," J. Metals, [7] 57-68 (1969).

12. Walker, R. D., and Anderson, D., "Reaction mechanisms in basic oxygen steelmaking Part 2," Iron and Steel, [8] 403-7 (1972).

13. McElroy, R., "Air release from mineral oils" (PhD Thesis), Dept. Pure and Appl. Chemistry, Univ. Strathclyde 1978.

14. Ross, S., and Suzin, Y., "Measurement of dynamic foam stability," Langmuir, **1**, 145-49 (1985).

15. Lin, R. C., and Phillips, G. F.,"Carbonated beverages," in: Encyclopedia of chemical processing and design (McKetta, J. J. and Cunningham, W. A., Ed.), Vol. 6, p.146-86, Marcel Dekker, Inc., New York and Basel, 1978.

16. Aubert, J. H., and Kraynik, A. M., and Rand, P. B.,"Aqueous foams," Sci. Amer., **254** 74-82 (1986).

17. Ilhan, A., and Hrma, P., "Foaming in glass melts under microgravity," Prog. Rept., Dept. Mater. Sci. Eng., Case Western Reserve Univ., submitted to NASA Lewis Research Center, Oct. 1987.

18. Monsalve, A., and Schechter, R. S., "The stability of foams: dependence of observation on the bubble size distribution," J. Coll. Interface Sci., **97**, 327-35 (1984).

19. Watkins, R. C., "An improved foam test for lubricating oils," J. Inst. Pet., **59**, 106-13 (1973).

20. Radoev, B. P., Schedulko, A. D., and Manev, E. D., "Critical thickness of thin liquid films: theory and experiment," J. Colloid Interface Sci., **95**, 254-65 (1983).

21. Ahmad, S. I., and Friberg, S., "Phase equilibria and stability in solutions of cationic surfactants," Acta Polytech. Scand., Chem. **102**, 3-14 (1971).

22. Friberg, S., "Liquid crystals and foams," in: Advances in liquid crystals (G. H. Brown, Ed.), Vol.3, p. 149-65. Academic Press, New York, 1978.

23. Hartland, S. and Barber, A. D., "A model for cellular foam,"Trans. Instn. Chem. Engrs., [52] 43 (1974).

24. Leonard, R. A., and Lemlich, R., "A study of interstitial liquid flow in foam," AIChE J., **11**, 18-29 (1965).

25. Hrma, P., "Model for steady foam blanket," J. Coll. Interface Sci., to be published.

26. Jebsen-Marwedel, H., and Dinger, K., "Equilibrium temperature of the concentration of gases in different molten glasses as a refining criterion," Verres Refr., [8] 19-25 (1947) in French.

27. Shaffer, E. W., "An improved technique for measuring reboil tendency in amber glasses," Annu. Conf. Glass Probl., 35th, 121-30 (1974).

28. Rosen, M. J., Surfactants and interfacial phenomena, p. 200-23. John Wiley & Sons, New York, 1978.

29. Kim, D.-S., and Hrma, P., "Volume changes during batch to glass conversion," to be published.

30. Hrma, P., "Bubble removal from molten glass," Proc. 15th International Congress on Glass, Leningrad, 1989.

31. Kim, D.-S., and Hrma, P., "Foaming in glass melts by sodium sulfate decomposition," to be published.

10. APPENDICES
Appendix I

According to the separation degree, transient foams can be classified as bulk foams or as surface foams. If bubbles grow quickly and move slowly, that is, $dr/dt >> v_B$, where dr/dt is the bubble growth rate and v_B the bubble velocity, spatially uniform bubble nucleation density will result in a bulk foam. Such a foam is stabilized against bubble segregation at the surface if the liquid drainage is slow, that is, $H_B >> vt_E$, where H_B is the mixture (liquid+foam) height, v the liquid velocity with respect to a foam cell (bubble), and t_E the experimental time. If, on the other hand, bubbles rise quickly to the surface, that is, $dr/dt << v$, a surface foam will be generated.

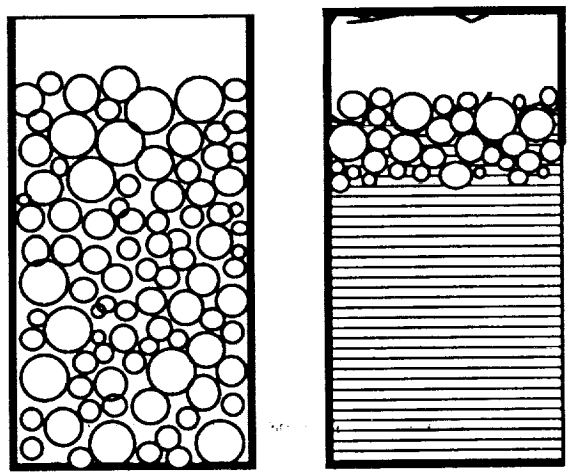

For bubble velocity and growth rate, the following formulas can be applied: $v_B \propto g\rho r^2/\eta$, where g is the gravity, ρ the density, and η the viscosity, and $dr/dt \propto D\Delta c/\delta$,where D is the diffusion coefficient, Δc the oversaturation, and δ the concentration layer thickness. Using the equation $\delta \propto (\eta D/g\rho)^{1/3}$, one can arrive at the following surface foam condition : $(\eta D/g\rho)^{2/3}\Delta c/r^2 << 1$. This condition indicates that surface foam cannot be produced without a separating force (such as gravity).

A bulk foam is converted into a surface foam if the liquid is quickly drained from the lamellae, that is, $H_B < vt_E$, and the bubble lifetime at the surface is sufficiently long. Cells do not expand by internal pressure if gas and liquid in cells within foam are in equilibrium ($\Delta c = 0$).

Appendix II

Capillary suction under microgravity: 2-D model

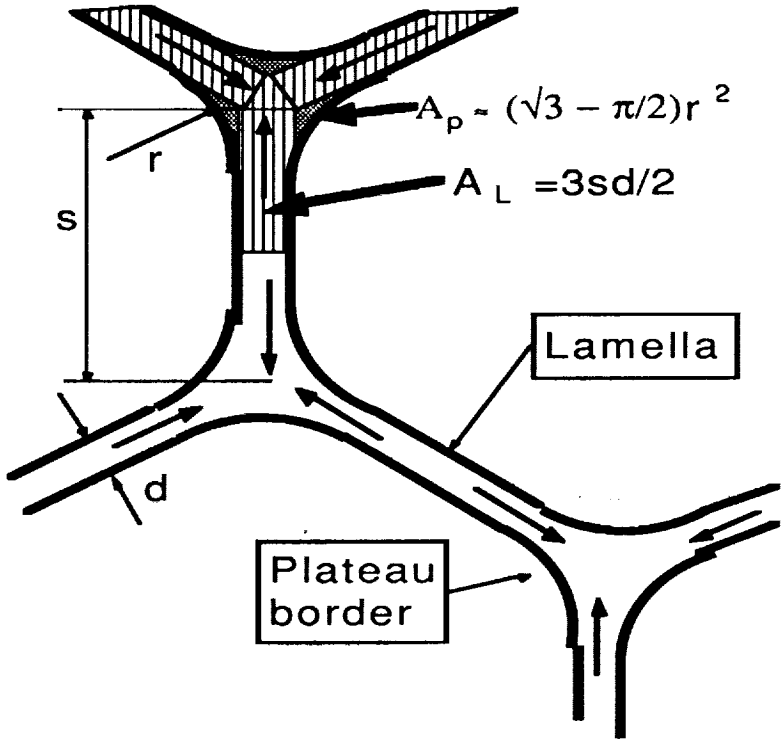

$$A = A_L + A_P = A_i = A_f$$

A_P	Plateau border area
A_L	half lamella area
i	initial
f	final
s	lamella length ($s_i = s_f = s$)
d	lamella thickness
r	Plateau border radius

$$3s(d_i - d_f) = (2\div 3 - p)(r_f^2 - r_i^2)$$

spherical foam condition: $2r_f > s$

for $d_i >> d_f$ and $r_f >> r_i$: $\quad d_i/s > 0.027$

Table 1: Forces acting in transient foams.

FORCE	REMARKS
VISCOUS DRAG	should be low for short time experiments
INTERNAL PRESSURE	should be smaller than gravity force
GRAVITY	dominates in low viscosity transient foams
CAPILLARITY	operates in non-spherical foams
ELECTROSTATIC FORCE *STERIC FORCE* *VAN DER WAALS FORCE* *GRAD* σ	operate in drained persistent foams

Table 2 a: Summary of foam generation methods.

METHOD	REMARKS
GAS ENTRAPMENT	initial conditions not well defined
BUBBLING	not suitable for microgravity
GAS RELEASE:	
SHAKING	initial conditions not well defined
PRESSURE DROP	
IN CONTAINER	sensitive to pressure fluctuations
CONTAINERLESS	large gas losses before foaming
NUCLEATION AGENT	
ADDITION	reasonable reproducibility

Table 2 b: Foam generation methods from gas-oversaturated liquids.

	GLASS MELT	AQUEOUS LIQUID
NUCLEATION	RESIDUAL SILICA GRAINS	SOLID PARTICLE ADDITION
OVERSATURATION	1) PRESSURE DECREASE AT CONSTANT TEMPERATURE 2) TEMPERATURE INCREASE AT CONSTANT PRESSURE	PRESSURE DECREASE

Table 3: High and low temperature foaming systems.

GLASS MELT
SODA-LIME GLASS
FOAMING AGENT: Na_2SO_4
NUCLEATION AGENT: SILICA SAND
T = 1350 - 1500°C
COLLAPSE TIME: ~400 SECONDS
AQUEOUS LIQUID (MODEL)
WATER WITH MILD SURFACTANT
FOAMING AGENT: CO_2
NUCLEATION AGENT: SOLID PARTICLES
GRANULAR ALUMINA
GLASS BEADS
METALLIC BALLS
ROOM TEMPERATURE
COLLAPSE TIME: ~10 SECONDS

Table 4: Correspondence between collapse susceptibility (n) and collapse behavior.

RANGE	TOP BUBBLE BEHAVIOR	COLLAPSE BEHAVIOR
$-\infty \leq n < 0$	long residence time	persistent foam
$n = 0$	r_B/t_B decreases with time	exponential collapse
$0 < n < 1$	t_B increases or r_B decreases with time, or both	collapse with a tail
$n = 1$	r_B/t_B = constant	linear collapse
$1 < n < \infty$	r_B increases by coalescence	catastrophic collapse

Table 5: Bubble burst frequency for sulfate foam in soda-lime glass.

T, °C	t_B, s	N, $g^{-1}s^{-1}$	N'
1400	4.0	0.6	30
1450	2.4	1.0	50
1500	1.5	1.7	85
1550	0.9	2.7	135

N NUMBER OF BURSTS PER UNIT MASS IN UNIT TIME ($N=A/\pi\, r_B^2\, M\, t_B$)

N' NUMBER OF BURSTS IN 10 g DURING 5 s.

Table 6: Summary of experimental variables for nucleation agent addition method.

VARIABLE	REMARKS
NUCLEATION AGENT	
AMOUNT	determines specific surface area
PARTICLE SIZE	optimum diameter for alumina 0.6 - 0.8 mm
	smaller particles agglomerate and float
ROUGHNESS	smooth particles lead to linear collapse
	rough particles: tendency to exponential collapse
DENSITY	heavy particles may cause gas losses from splashing
	light particles tend to float
SOLUBILITY	no significant effect
COATING OF CONTAINERS	
COATING AGENT	among alcohol based (Rain-X) and oil based (Triflow
	and 711) agents, 711 resulted in the best reproducibility
PROCEDURE	cleaning, one-layer coating, room temperature drying
DROPPING TECHNIQUE	
DROPPING HEIGHT	depends on particle weight
	too high: gas losses
	too low: nozzle wetting and clogging
NOZZLE DIAMETER	optimum: instantaneous dropping, minimum scatter

Table 7: Summary of experimental conditions and collapse behavior for nucleation agent addition method.

Exp	Addition		Coating	Height	Linear		Exponential	
No	Material	Wt.	Agent	Max - Min	Intercept	Coefficent	Intercept	Coefficent
		(g)		(mm)	(mm)	(mm/s)	(mm)	(s^-1)
A31	Alumina	0.30	711	05.98	33.70	0.433	2.63	0.137
A32	Alumina	0.30	711	04.83	31.60	0.385	2.27	0.144
A33	Alumina	0.30	711	06.21	33.05	0.560	2.25	0.147
Average				**05.67**	**32.78**	**0.460**	**2.38**	**0.143**
St. Dev.				**00.74**	**1.08**	**0.090**	**0.21**	**0.005**
A34	Alumina	0.30	none	09.20	37.01	0.838	3.13	0.229
A35	Alumina	0.30	none	08.28	37.05	0.711	2.75	0.137
A36	Alumina	0.30	none	06.44	34.22	0.552	2.53	0.153
Average				**07.97**	**36.09**	**0.700**	**2.64**	**0.145**
St. Dev.				**01.41**	**1.62**	**0.143**	**0.16**	**0.011**
A37	Alumina	0.70	711	27.12	67.31	1.956	4.18	0.122
A38	Alumina	0.70	711	31.92	72.67	1.838	4.63	0.122
A39	Alumina	0.70	711	32.88	70.50	1.919	4.25	0.113
Average				**30.64**	**70.16**	**1.904**	**4.35**	**0.119**
St. Dev.				**03.09**	**2.70**	**0.061**	**0.24**	**0.005**
A40	Gra. Brick	0.50	711	12.72				
A41	Gra. Brick	0.50	711	12.96				
A42	Gra. Brick	0.50	711	18.24				
Average				**14.64**				
St. Dev.				**03.12**				
A43	Alumina	0.70	711	33.80	81.08	3.808	4.73	0.195
A44	Alumina	0.70	711	31.18	74.62	3.692	4.47	0.201
A45	Alumina	0.70	711	21.19	59.02	2.516	4.10	0.207
Average				**28.72**	**71.57**	**3.339**	**4.43**	**0.201**
St. Dev.				**06.65**	**11.34**	**0.715**	**0.32**	**0.006**
A46	Alumina	0.70	711	33.64	76.30	4.757	4.45	0.250
A47	Alumina	0.70	711	31.95	73.83	3.976	4.57	0.240
*A48**	Alumina	0.70	711	*20.33*	*90.93*	*2.088*	*6.31*	*0.155*
Average				**32.80**	**75.06**	**4.366**	**4.51**	**0.245**
St. Dev.				**01.20**	**1.75**	**0.552**	**0.08**	**0.007**
A49	Alumina	0.70	711	26.84	65.57	3.920	4.17	0.258
A50	Alumina	0.70	711	24.69	65.16	3.741	4.22	0.259
A51	Alumina	0.70	711	31.22	73.81	4.105	4.60	0.256
Average				**27.58**	**68.18**	**3.922**	**4.33**	**0.258**
St. Dev.				**03.33**	**4.88**	**0.182**	**0.24**	**0.002**
A52	Glass Beads	1.00	Rain-X	24.54	64.16	2.427	4.97	0.261
A53	Glass Beads	1.00	Rain-X	21.24	59.99	2.148	4.76	0.261
A54	Glass Beads	1.00	Rain-X	20.77	60.79	2.478	4.72	0.275
Average				**22.18**	**61.65**	**2.351**	**4.82**	**0.266**
St. Dev.				**02.05**	**02.21**	**0.178**	**0.13**	**0.008**
A55	Glass Beads	1.00	Rain-X	27.54	75.62	5.411	5.64	0.483
A56	Glass Beads	1.00	Rain-X	23.16	64.58	4.314	5.35	0.513
A57	Glass Beads	1.00	Rain-X	23.16	66.07	5.337	5.03	0.547
Average				**24.62**	**68.76**	**5.021**	**5.34**	**0.514**
St. Dev.				**02.53**	**05.99**	**0.613**	**0.31**	**0.032**
A58	Glass Beads	1.00	Rain-X	09.01	41.12	1.483	3.37	0.294
A59	Glass Beads	1.00	Rain-X	08.04	40.21	1.462	3.11	0.288
A60	Glass Beads	1.00	Rain-X	09.51	42.18	1.593	3.29	0.281
Average				**08.85**	**41.17**	**1.513**	**3.26**	**0.288**
St. Dev.				**00.75**	**0.98**	**0.070**	**0.13**	**0.007**

Table 7: (con't) Summary of experimental conditions and collapse behavior for nucleation agent addition method.

Exp	Addition		Coating	Height	Linear		Exponential	
No	Material	Wt.	Agent	Max - Min	Intercept	Coefficent	Intercept	Coefficent
		(g)		(mm)	(mm)	(mm/s)	(mm)	(s^-1)
A61	Glass Beads	1.20	Rain-X	22.31	60.20	2.494	4.64	0.285
A62	Glass Beads	1.20	Rain-X	13.88	47.54	1.570	3.98	0.287
A63	Glass Beads	1.20	Rain-X	15.87	53.08	2.281	3.93	0.285
A64	Glass Beads	1.20	Rain-X	21.32	59.58	2.713	4.46	0.294
A65	Glass Beads	1.20	Rain-X	17.35	53.41	2.391	3.98	0.302
A66	Glass Beads	1.20	Rain-X	09.67	43.92	1.611	3.38	0.300
Average				**16.73**	**52.95**	**2.177**	**4.06**	**0.292**
St. Dev.				**04.72**	**6.44**	**0.476**	**0.45**	**0.008**
A67	Alumina	0.70	Rain-X	31.93	67.57	2.353	4.91	0.197
A68	Alumina	0.70	Rain-X	34.85	78.58	2.837	5.20	0.193
A69	Alumina	0.70	Rain-X	32.17	70.45	2.152	5.29	0.189
Average				**32.98**	**72.20**	**2.448**	**5.13**	**0.193**
St. Dev.				**01.62**	**05.71**	**0.352**	**0.20**	**0.004**
A70	Glass Beads	1.20	Rain-X	20.47	63.53	4.728	4.48	0.407
A71	Glass Beads	1.20	Rain-X	15.35	50.43	2.416	4.54	0.414
A72	Glass Beads	1.20	Rain-X	15.35	51.25	2.900	4.27	0.430
Average				**17.06**	**55.07**	**3.348**	**4.43**	**0.417**
St. Dev.				**02.96**	**7.34**	**1.219**	**0.14**	**0.012**
A73	Met. Balls	20.40	Rain-X	29.00	81.96	3.838	4.81	0.271
A74	Met. Balls	20.40	Rain-X	22.66	65.76	2.756	4.49	0.280
A75	Met. Balls	20.40	Rain-X	14.86	56.12	2.120	4.03	0.279
Average				**22.17**	**67.95**	**2.905**	**4.44**	**0.277**
St. Dev.				**07.08**	**13.06**	**0.869**	**0.39**	**0.005**
A76	Met. Balls	20.40	Rain-X	33.42	73.71	2.782	4.36	0.197
A77	Met. Balls	20.40	Rain-X	27.77	66.53	2.308	4.30	0.204
A78	Met. Balls	20.40	Rain-X	33.92	72.48	2.392	4.60	0.205
A79	Met. Balls	20.40	Rain-X	22.86	60.76	2.229	4.36	0.272
Average				**29.49**	**68.37**	**2.428**	**4.41**	**0.202**
St. Dev.				**05.23**	**05.97**	**0.245**	**0.13**	**0.004**
A80	Met. Balls	20.40	711	19.17	57.33	2.433	3.70	0.230
A81	Met. Balls	20.40	711	24.57	64.39	2.055	4.55	0.229
A82	Met. Balls	20.40	711	36.86	78.07	2.783	4.80	0.206
A83	Met. Balls	20.40	711	20.15	60.52	2.296	3.93	0.228
Average				**25.19**	**65.08**	**2.392**	**4.25**	**0.223**
St. Dev.				**08.13**	**09.13**	**0.304**	**0.52**	**0.012**

Table 8: Average collapse coefficients for nucleation agent addition method.

Trial No	No. of Exp's	Nucleation Agent	Grain Size (μm)	Mass (g)	Coating Agent	Foam Height* (mm)	Collapse Coefficient Linear** (mm/s)	Stand. Dev. (mm/s)	Exponential*** (mm/s)	Stand. Dev. (mm/s)
01	3	Alumina	600-841	0.30	711	05.67	0.460	0.090	0.143	0.005
02	3	Alumina	600-841	0.30	none	07.97	0.700	0.143	0.145	0.011
03	3	Alumina	600-841	0.70	711	30.64	1.904	0.061	0.119	0.005
04	3	Gra. Brick	600-841	0.50	711	14.64				
05	3	Alumina	600-841	0.70	711	28.72	3.339	0.715	0.201	0.006
06	2	Alumina	600-841	0.70	711	32.80	4.366	0.552	0.245	0.007
07	3	Alumina	600-841	0.70	711	27.58	3.922	0.182	0.258	0.002
08	3	Glass Beads	100-170	1.00	Rain-X	22.18	2.351	0.178	0.266	0.008
09	3	Glass Beads	100-170	1.00	Rain-X	24.62	5.021	0.613	0.514	0.032
10	3	Glass Beads	100-170	1.00	Rain-X	08.85	1.513	0.070	0.288	0.007
11	6	Glass Beads	100-170	1.20	Rain-X	16.73	2.177	0.476	0.292	0.008
12	3	Alumina	600-841	0.70	Rain-X	32.98	2.448	0.352	0.193	0.004
13	3	Glass Beads	100-170	1.20	Rain-X	17.06	3.348	1.219	0.417	0.012
14	3	Met. Balls	5000	20.40	Rain-X	22.17	2.905	0.869	0.277	0.005
15	4	Met. Balls	5000	20.40	Rain-X	29.49	2.428	0.245	0.202	0.004
16	4	Met. Balls	5000	20.40	711	25.19	2.392	0.304	0.223	0.012

* maximum height increase by gas liberation

** evaluated as dH/dt from the linear section of the collapse curve

*** evaluated as dlnH/dt from the linear section of the lnH vs. t curve

Table 9: Comparison of transient aqueous foams generated by pressure decrease method and nucleation agent addition method.

	PRESSURE DROP METHOD	NUCLEATION AGENT ADDITION METHOD
GENERATION TIME, s	1 - 2	2 - 3
COLLAPSE TIME, s	4 - 5	6 - 15
COLLAPSE RATE, mm/s	4 - 6	2 - 5
CELL RADIUS, mm	0.5	0.05
r_B, mm	0.6	0.6
n	2	1.7×10^3
m	1	11

n NUMBER OF COALESCING BUBBLES

m NUMBER OF COALESCENCE EVENTS

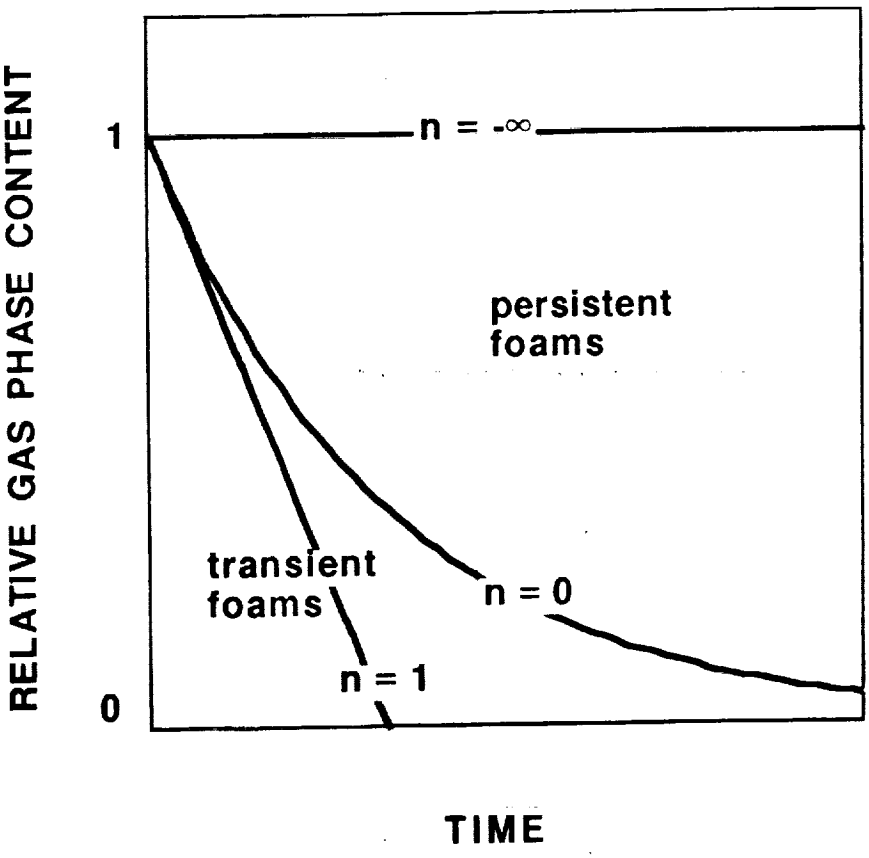

Figure 1: Range of collapse behavior for instantaneous foam.

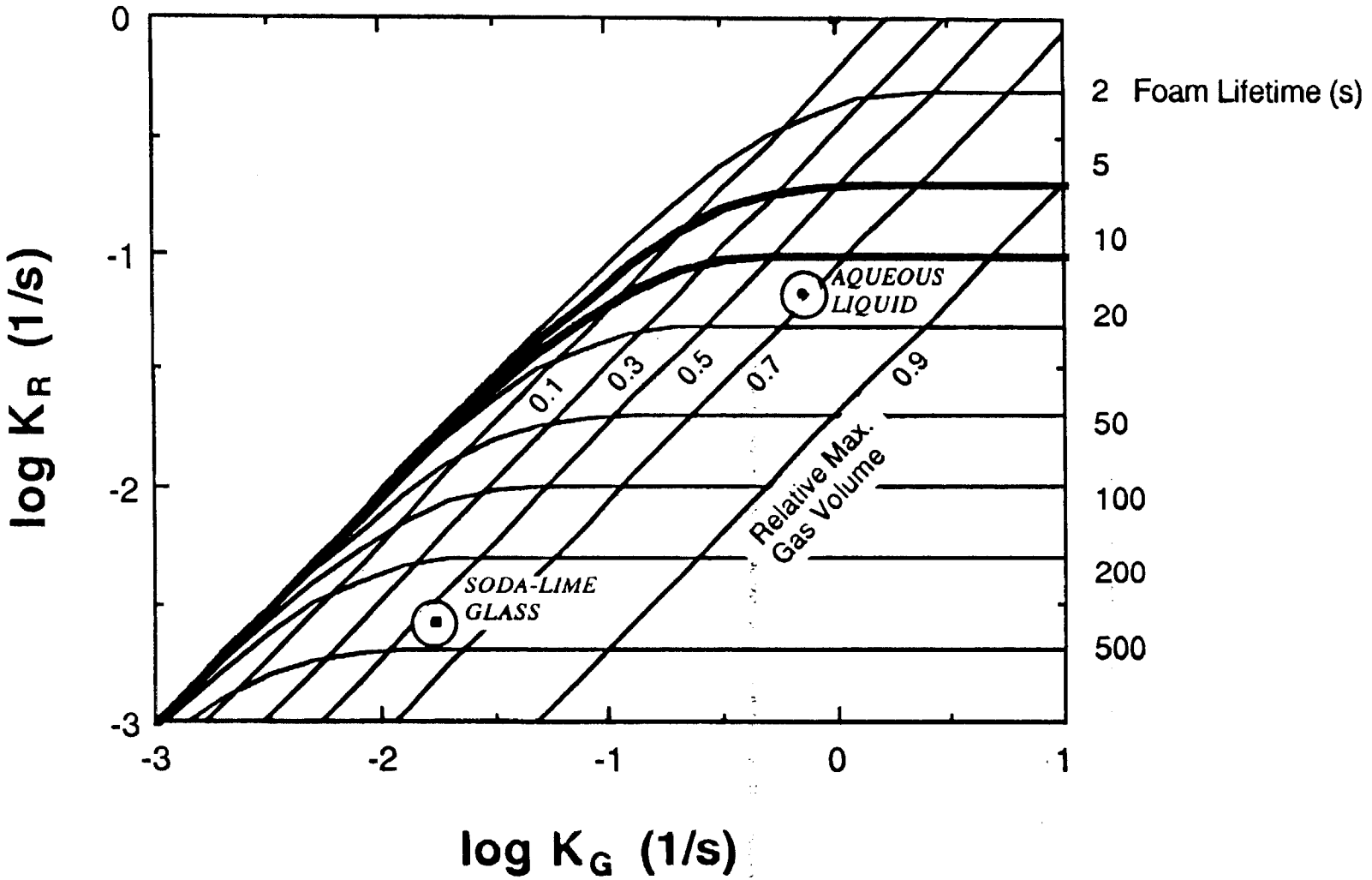

Figure 2: Map of lifetimes and maximum relative gas phase volume on the kinetic rate coefficient space for glass and aqueous foams.

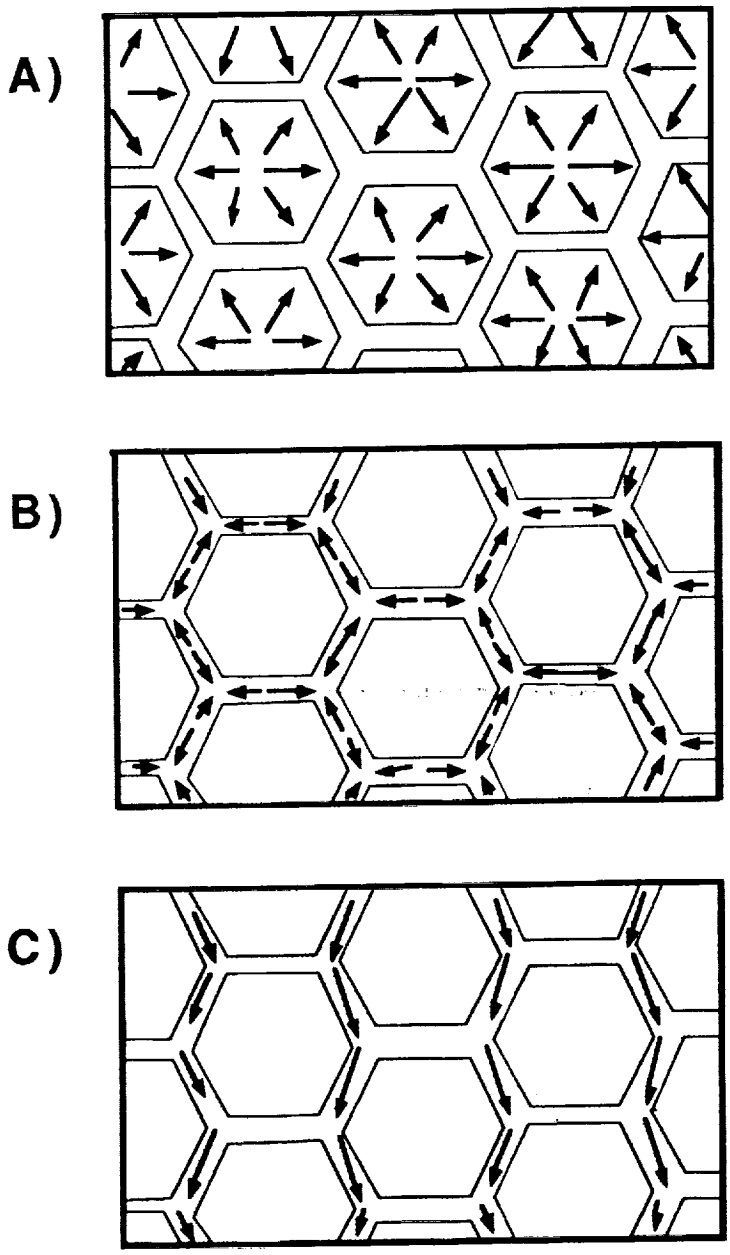

Figure 3: Schematic of action of forces in foam: (a) pressure force, (b) capillary suction, and (c) gravity.

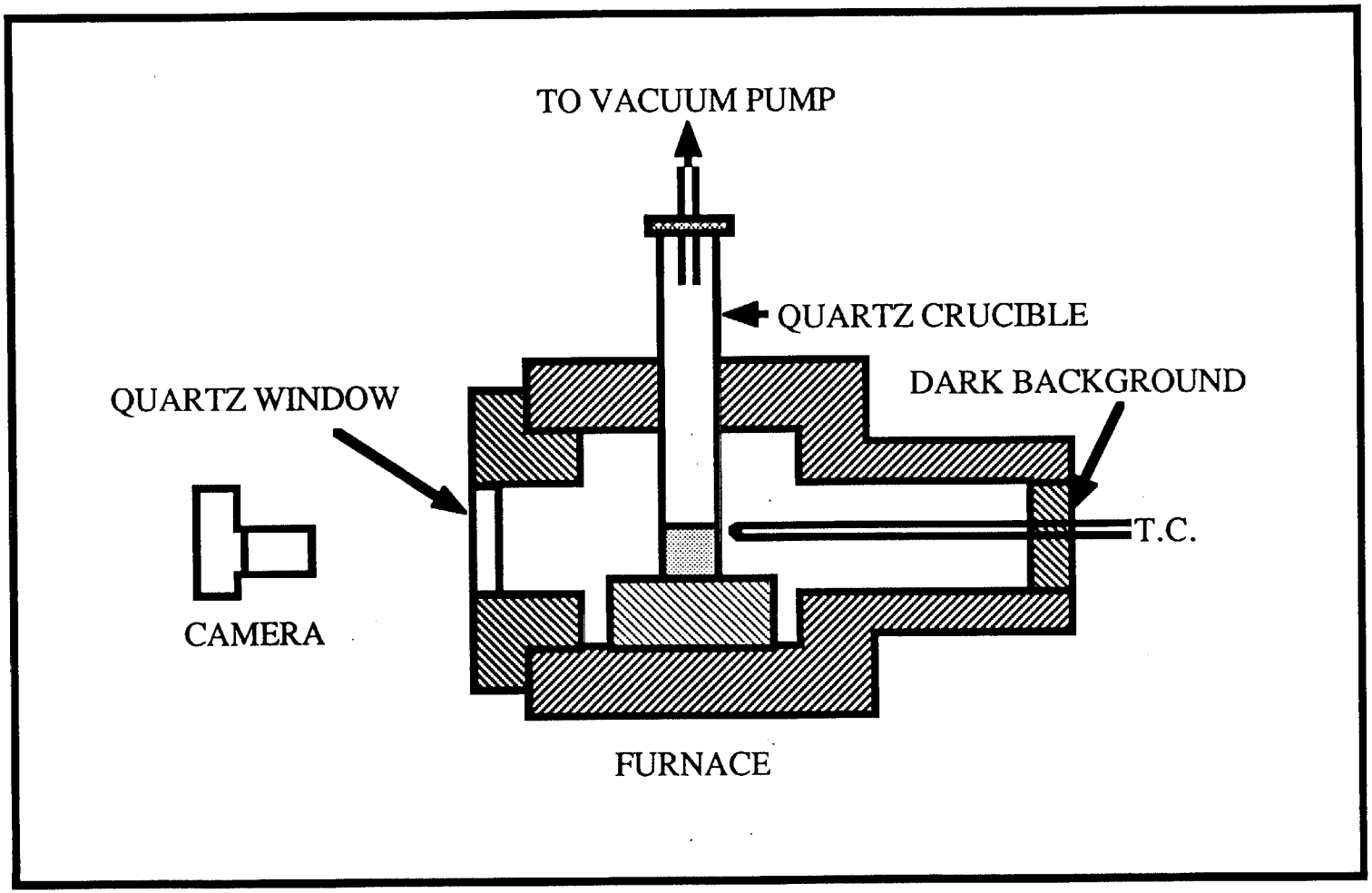

Figure 4: Reduced pressure furnace for glass foaming experiments.

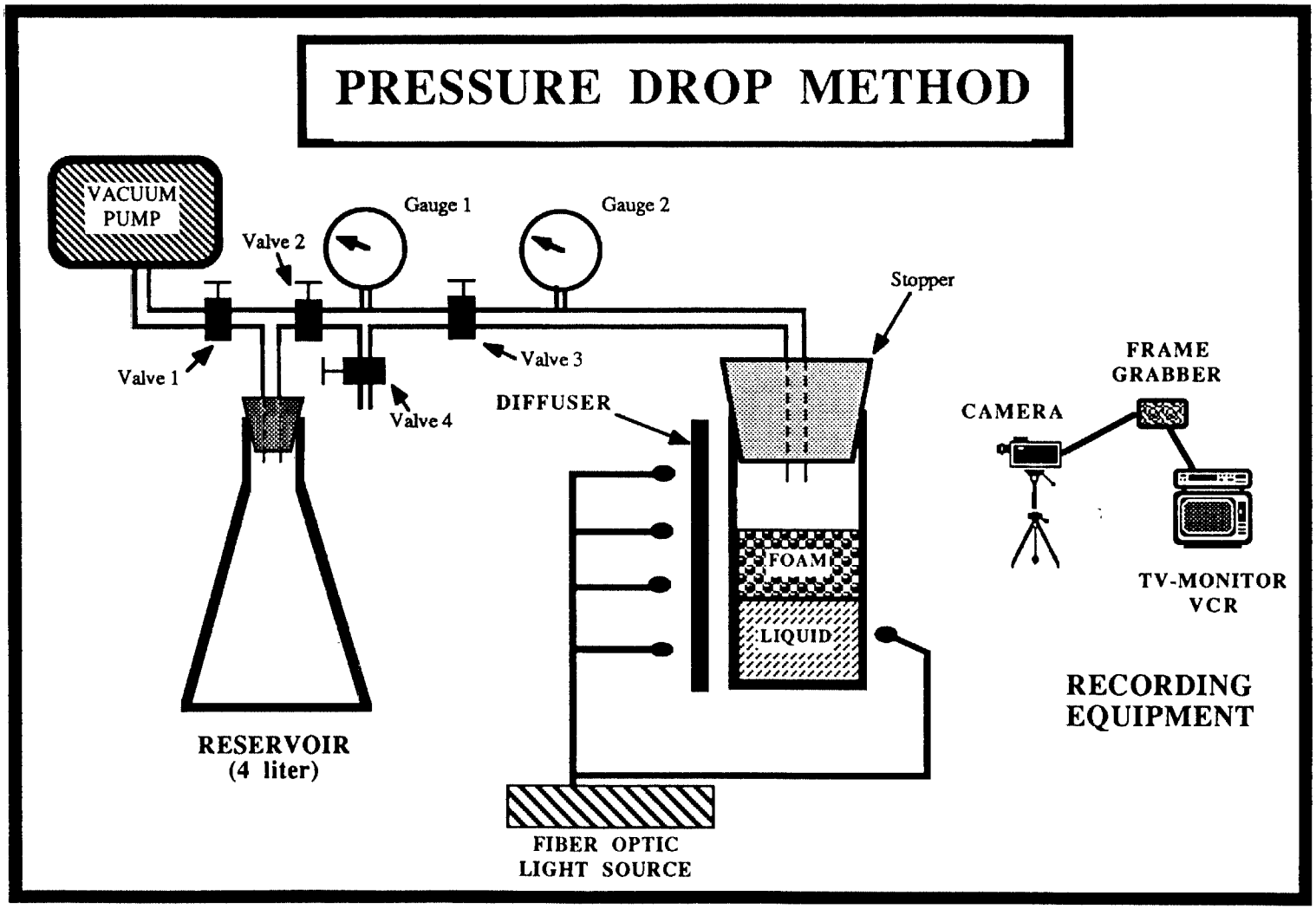

Figure 5: Experimental set-up for pressure decrease method.

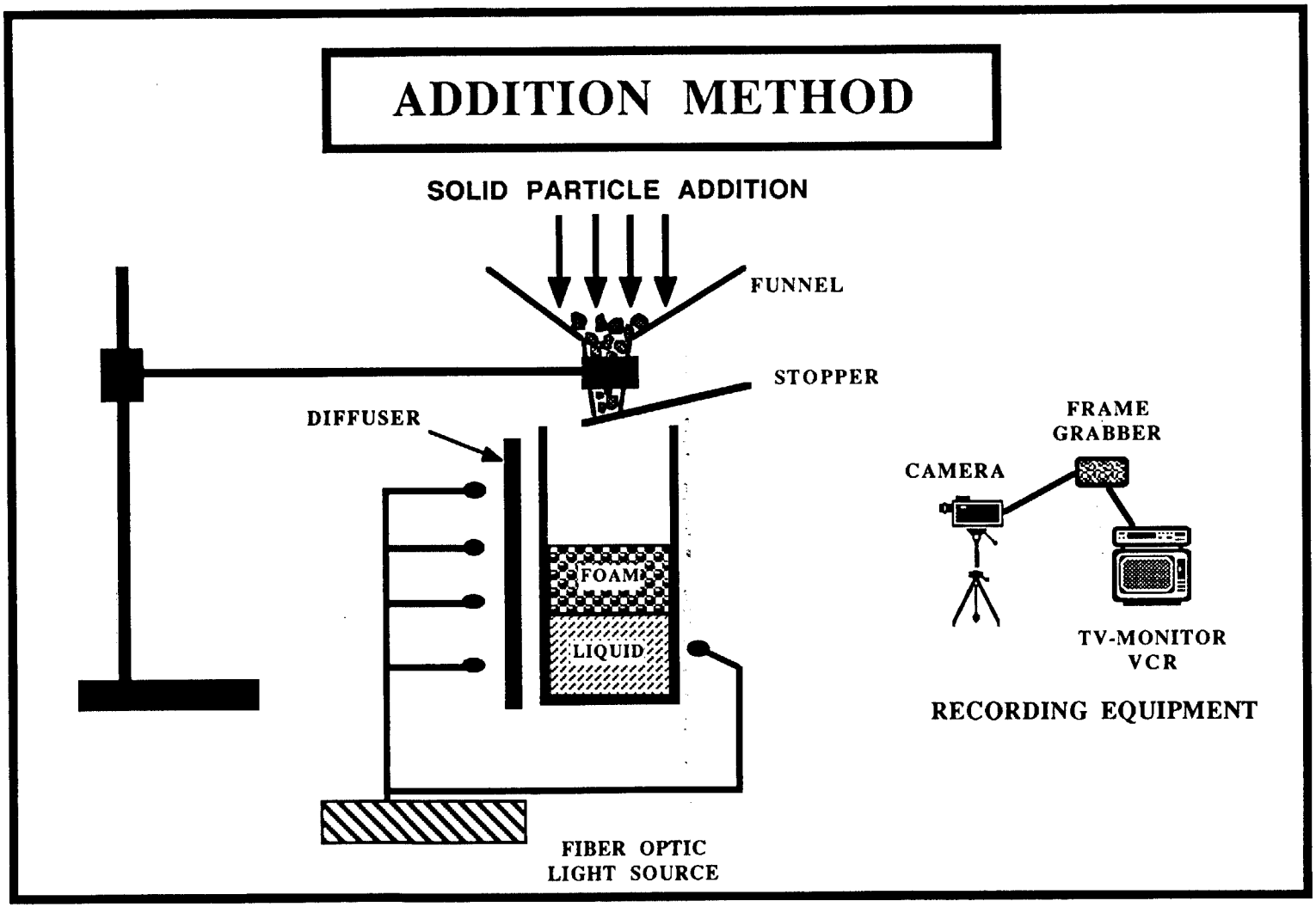

Figure 6: Experimental set-up for nucleation agent addition method.

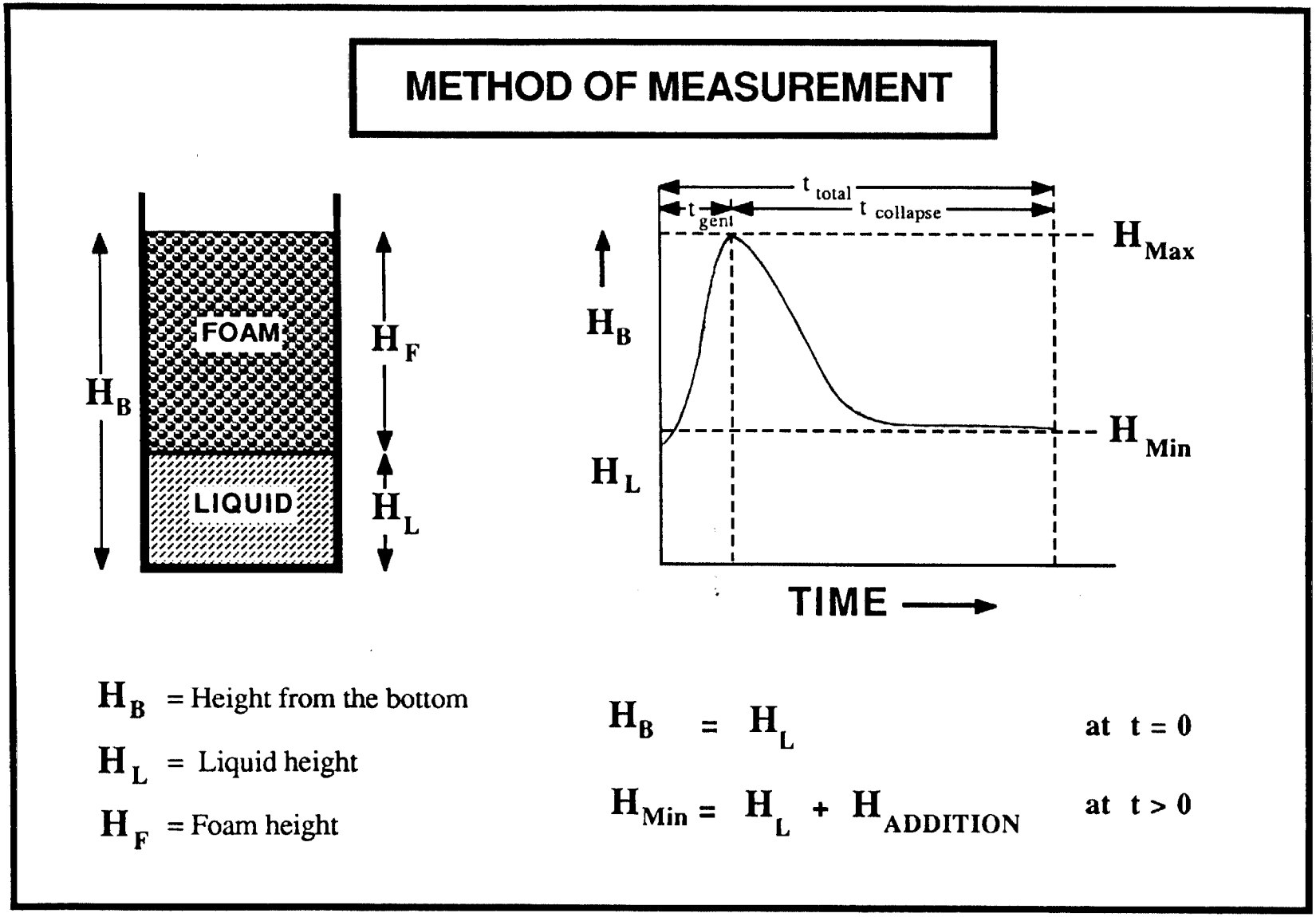

Figure 7: Measurement technique for foam height.

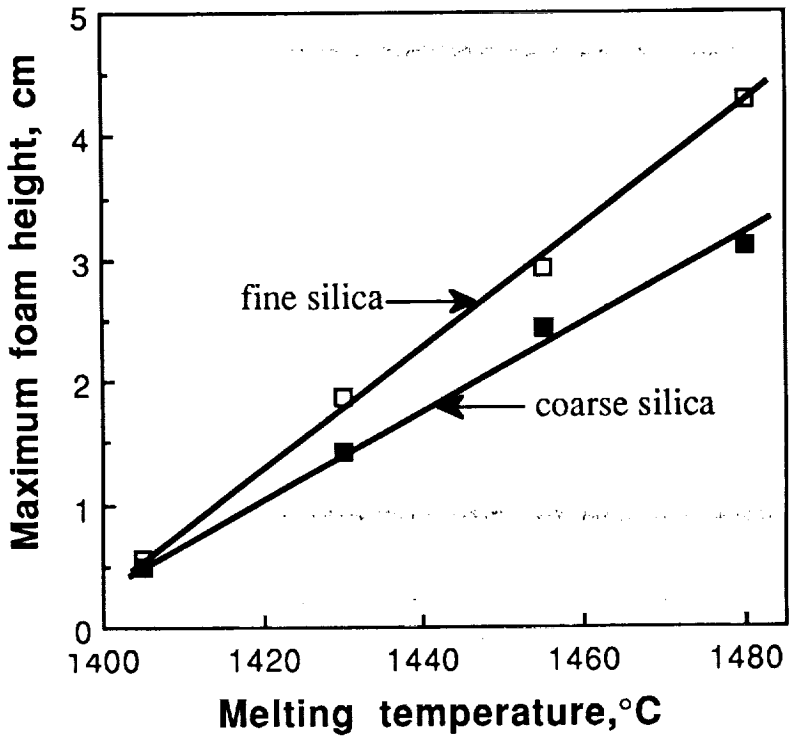

Figure 8: Effect of melting temperature and initial silica grain size on maximum foam height for batches containing 4% of total Na_2O from Na_2SO_4 and isothermally heated under atmospheric pressure.

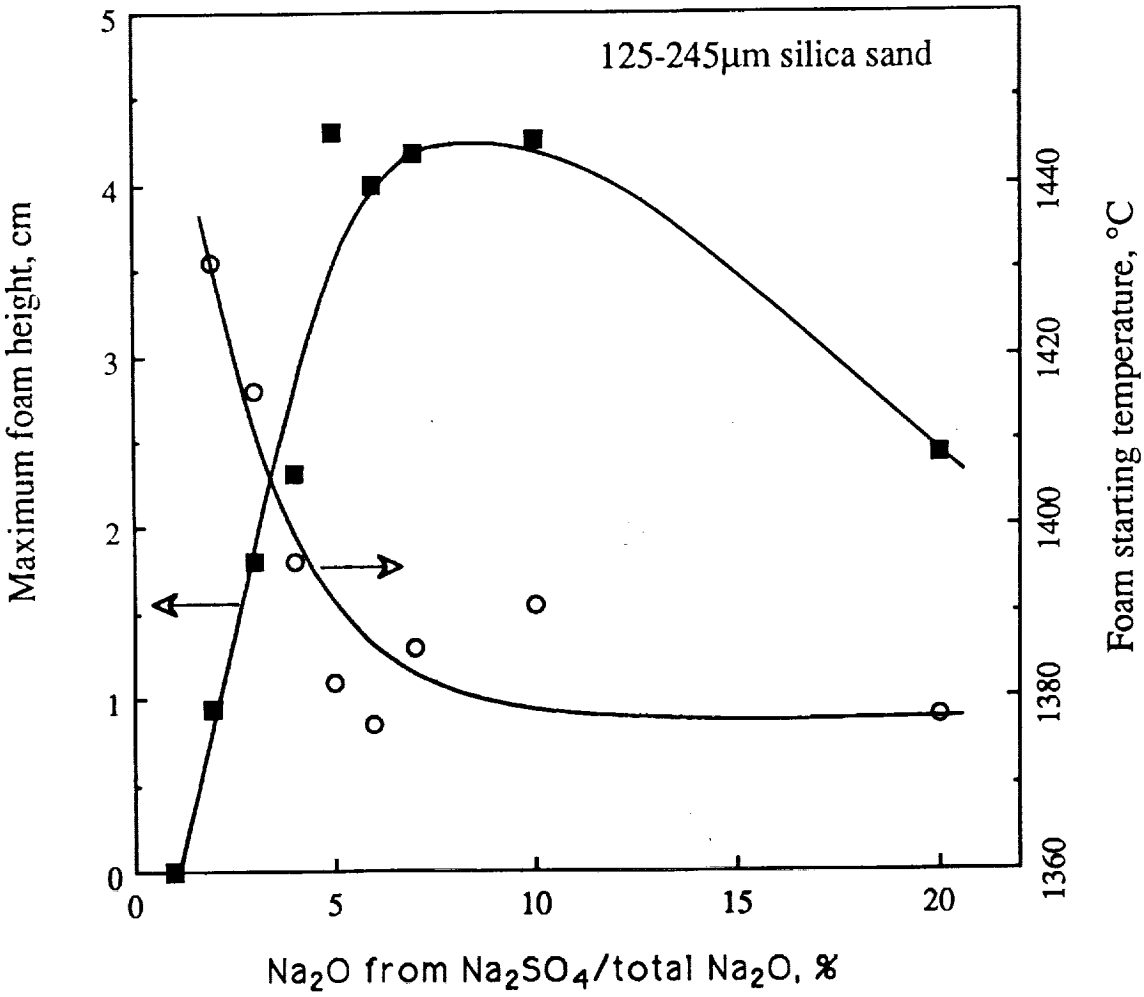

Figure 9: The effect of the initial sulfate concentration on the maximum foam height and foam starting temperature for coarse silica batches ramp heated at 14°C/min.

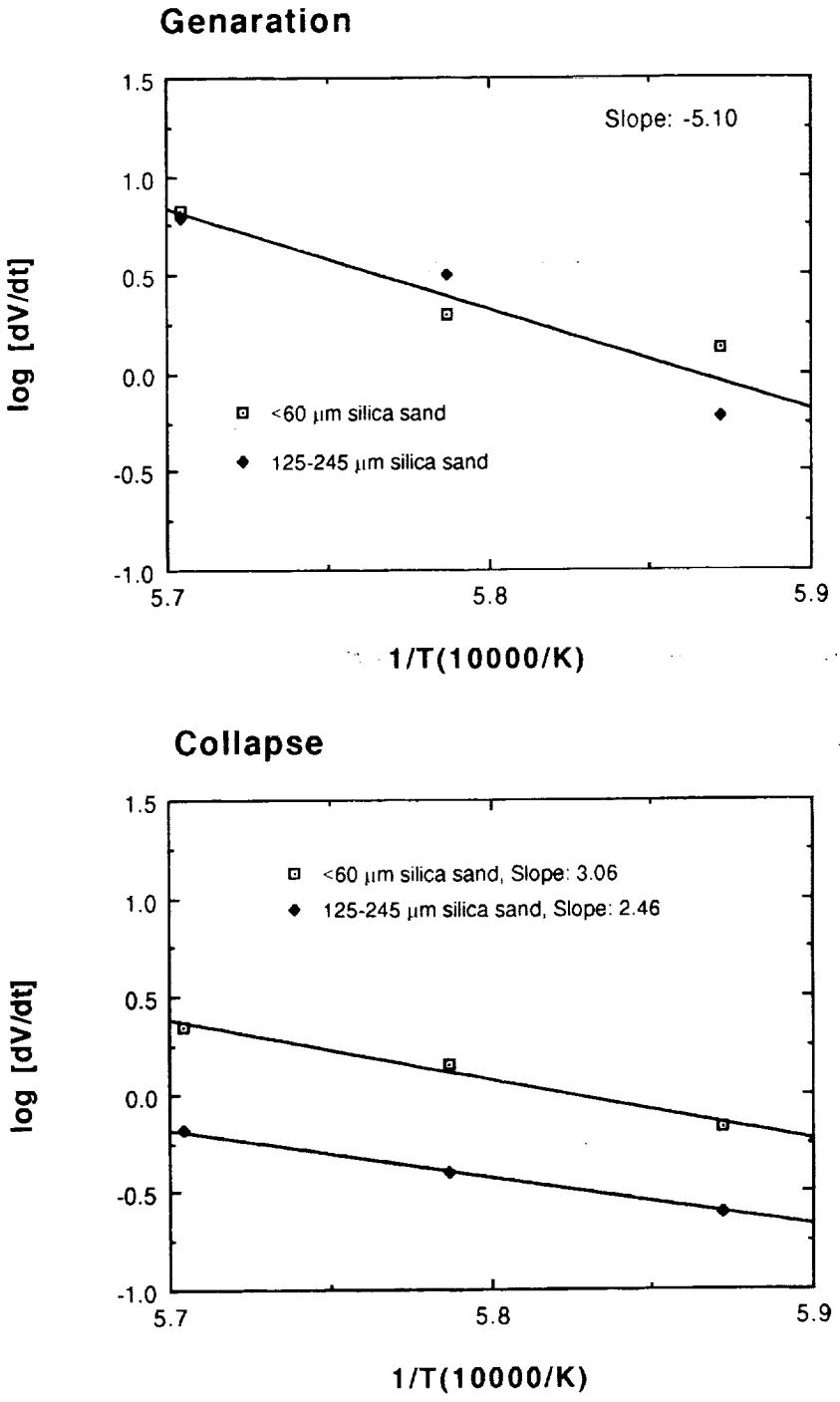

Figure 10: Effect of melting temperature and initial silica grain size on rate of change in foam volume, V, for batches containing 4% of total Na_2O from Na_2SO_4 and isothermally heated under atmospheric pressure.

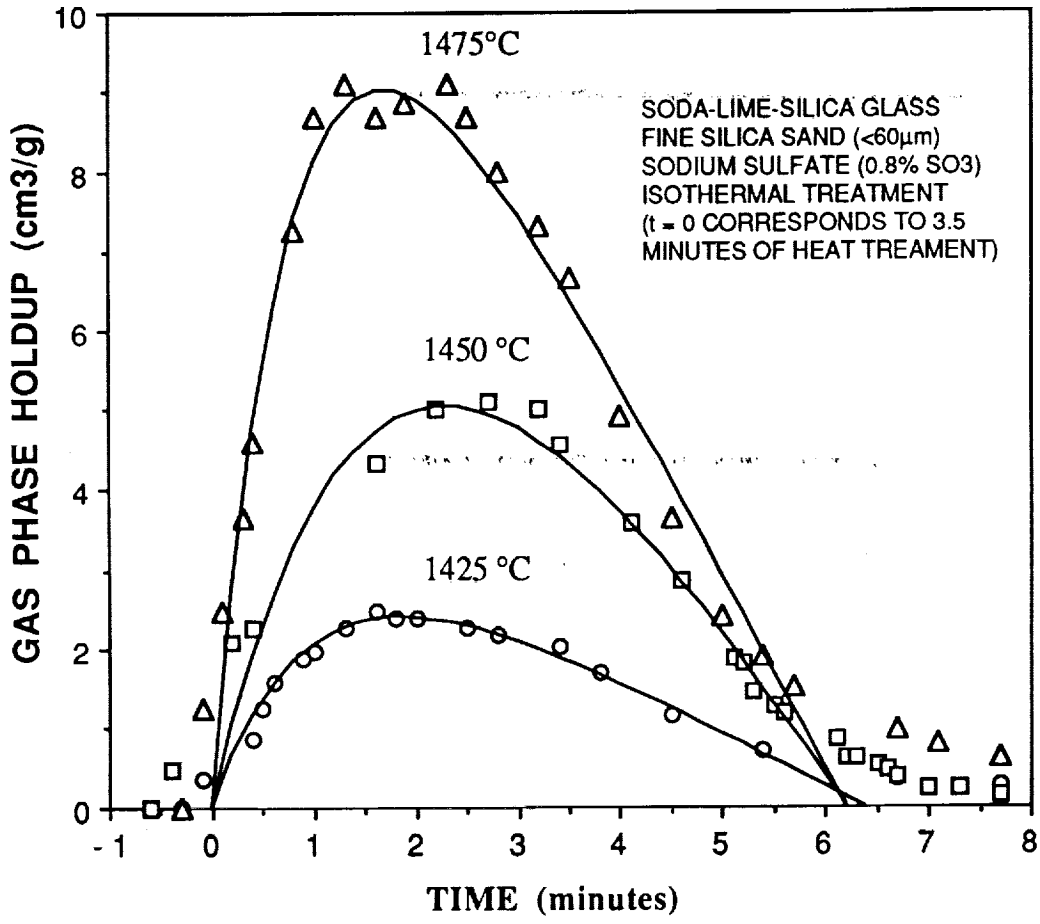

Figure 11: Gas phase holdup vs. time in 20 g of soda-lime glass with 4% of total Na_2O from Na_2SO_4, isothermally treated. The line was fitted by Eq. 9.

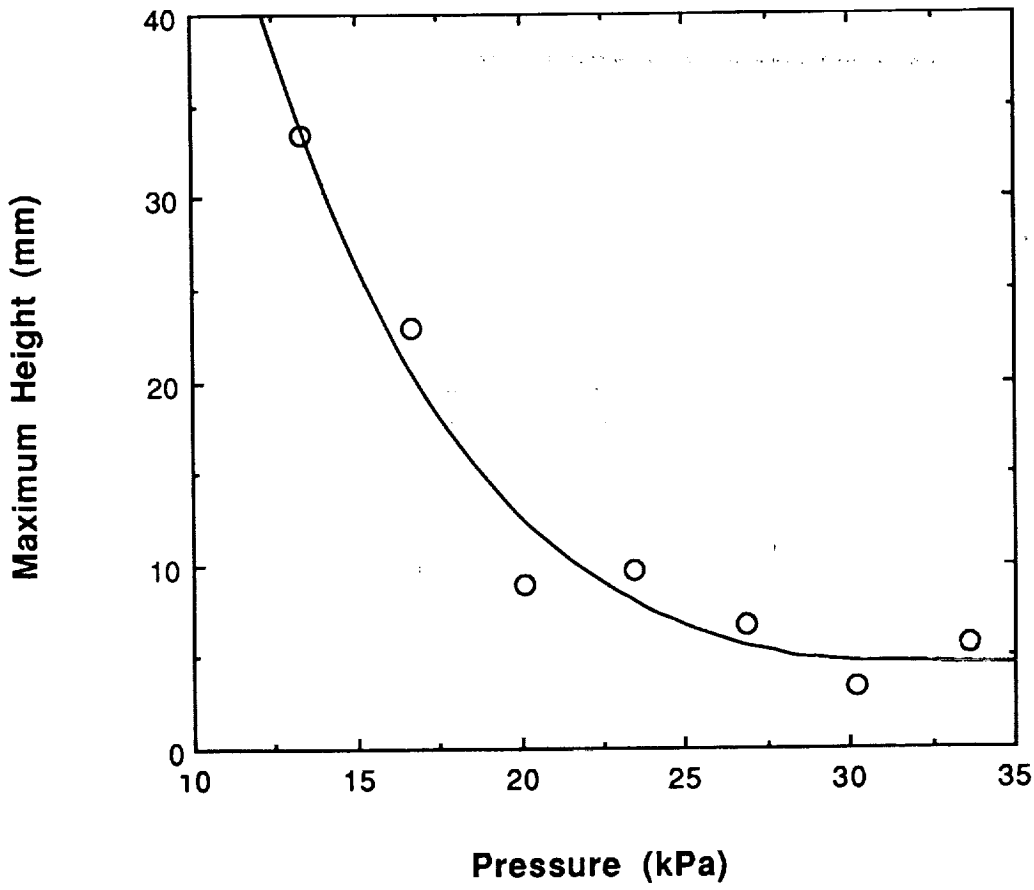

Figure 12: Maximum foam height vs. pressure for aqueous transient foam with pressure decrease method.

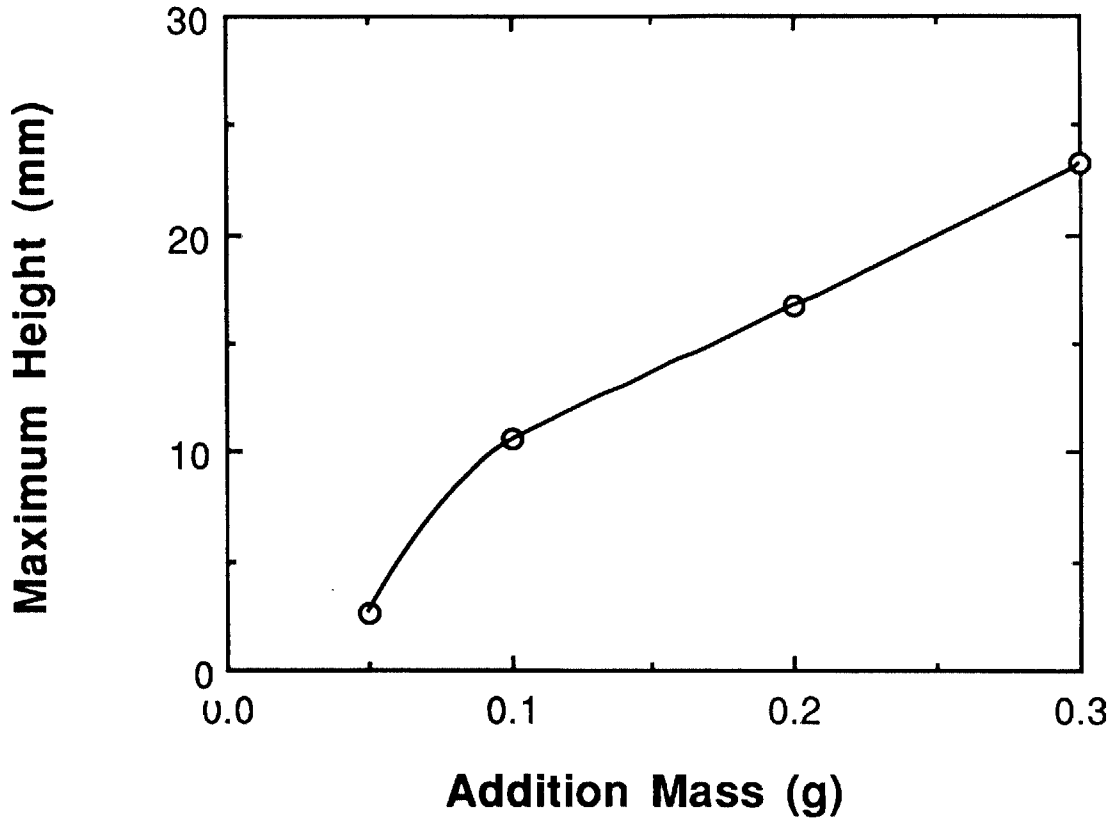

Figure 13: Maximum height vs. nucleation agent mass for aqueous transient foam generated by nucleation agent addition method with sugar as the nucleation agent.

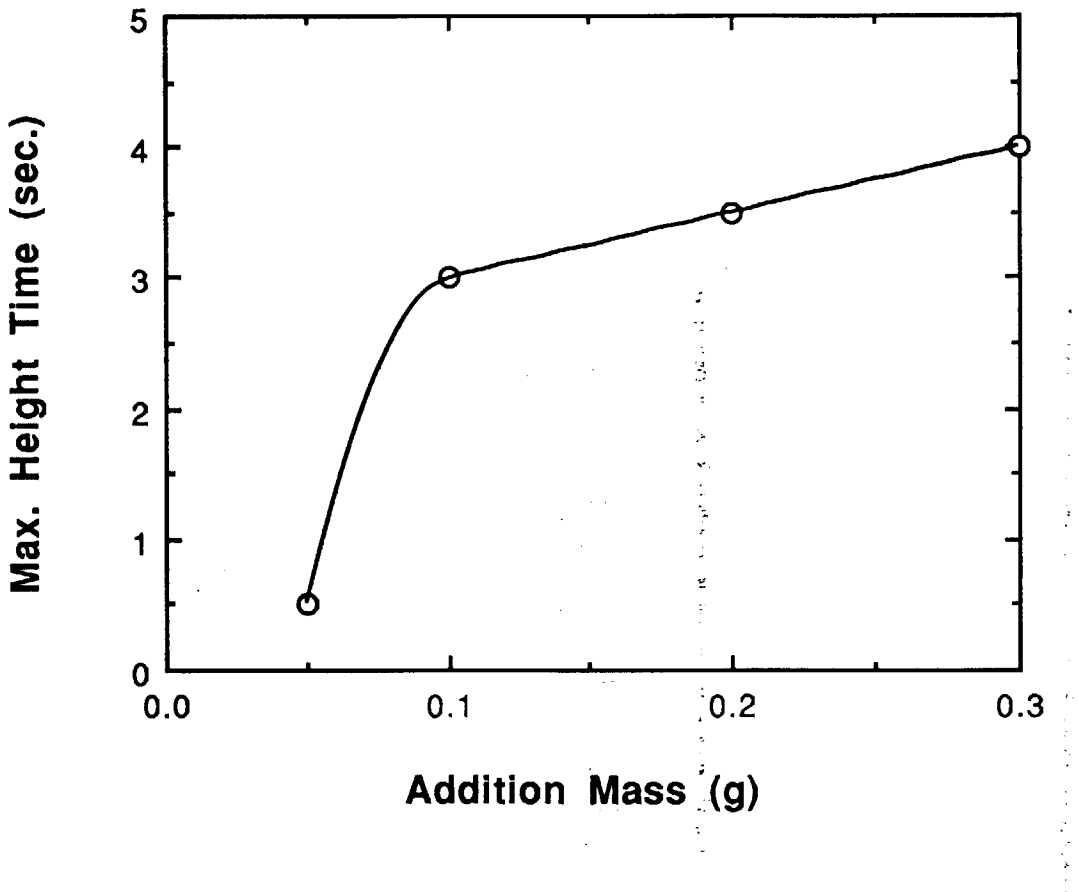

Figure 14: Maximum height time vs. nucleation agent mass for aqueous transient foam generated by nucleation agent addition method with sugar as the nucleation agent.

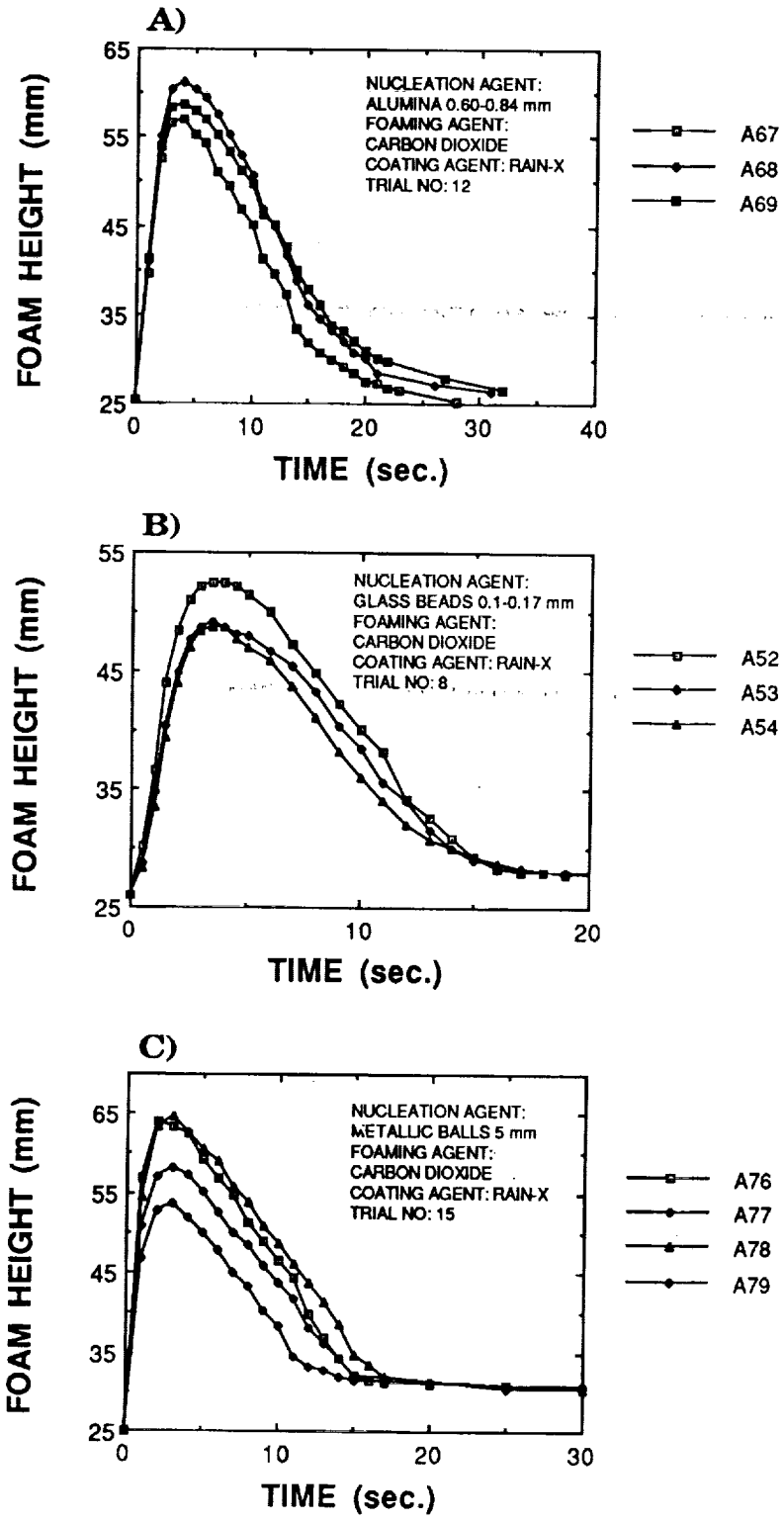

Figure 15: Foam height vs. time for aqueous transient foam generated by nucleation agent addition method with three nucleation agents: (a) alumina, (b) glass beads, and (c) metallic balls.

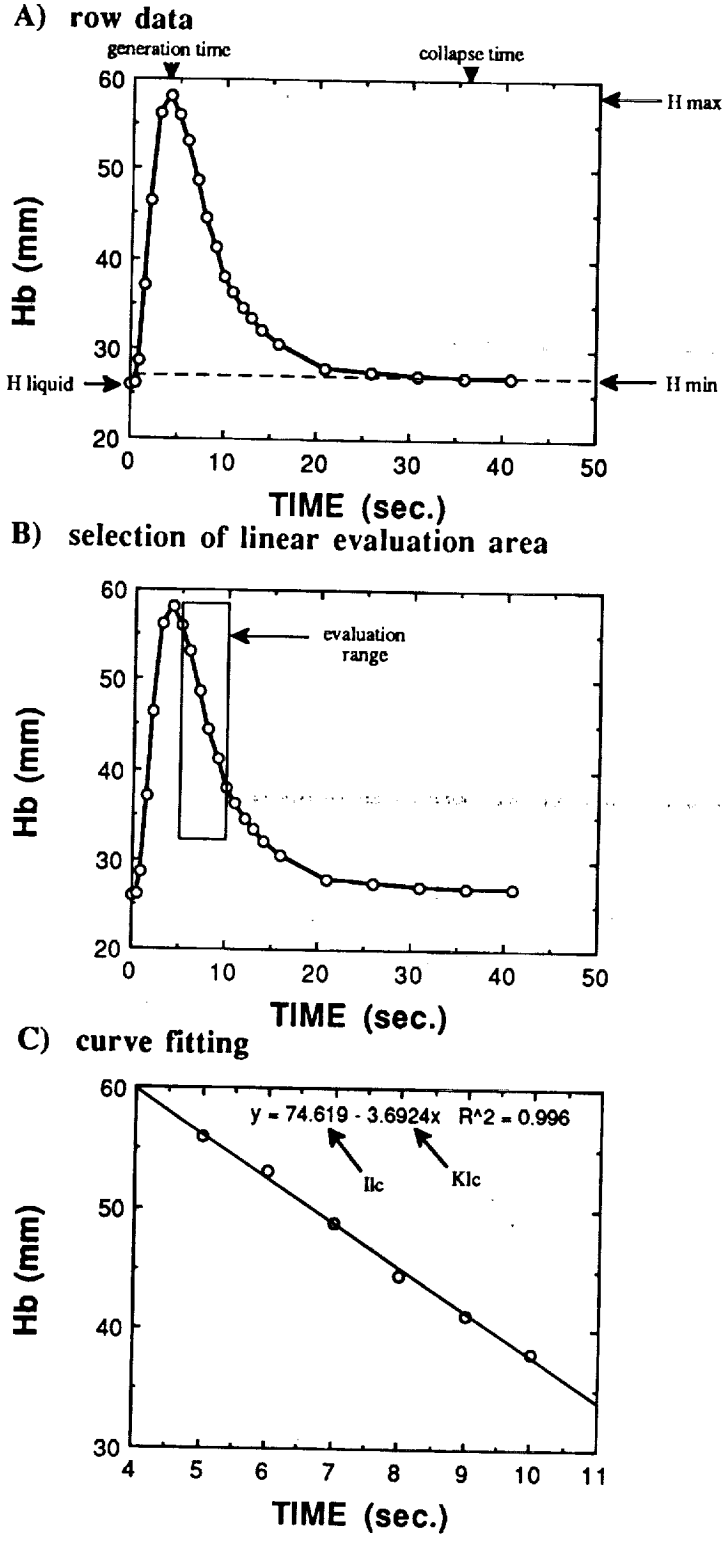

Figure 16: Schematic of evaluation procedure for linear collapse coefficient.

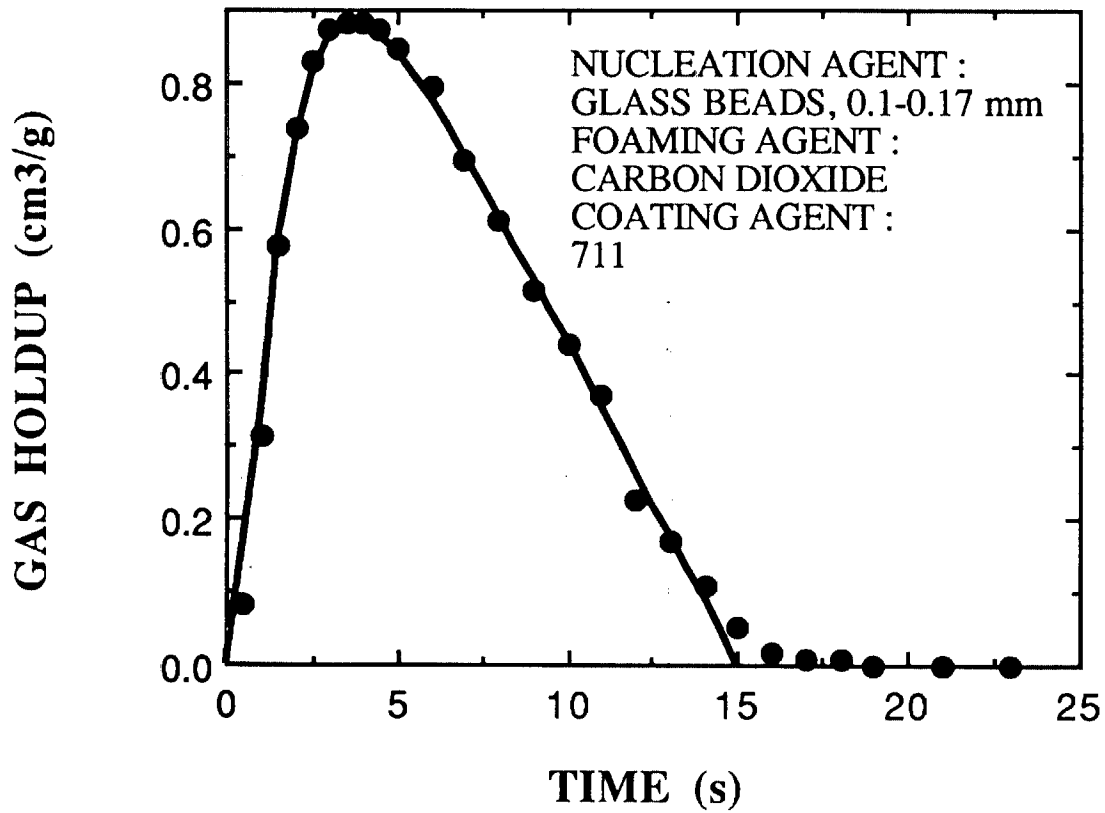

Figure 17: Gas holdup vs. time for aqueous transient foam with glass beads addition. The line was fitted by Eq. 9.

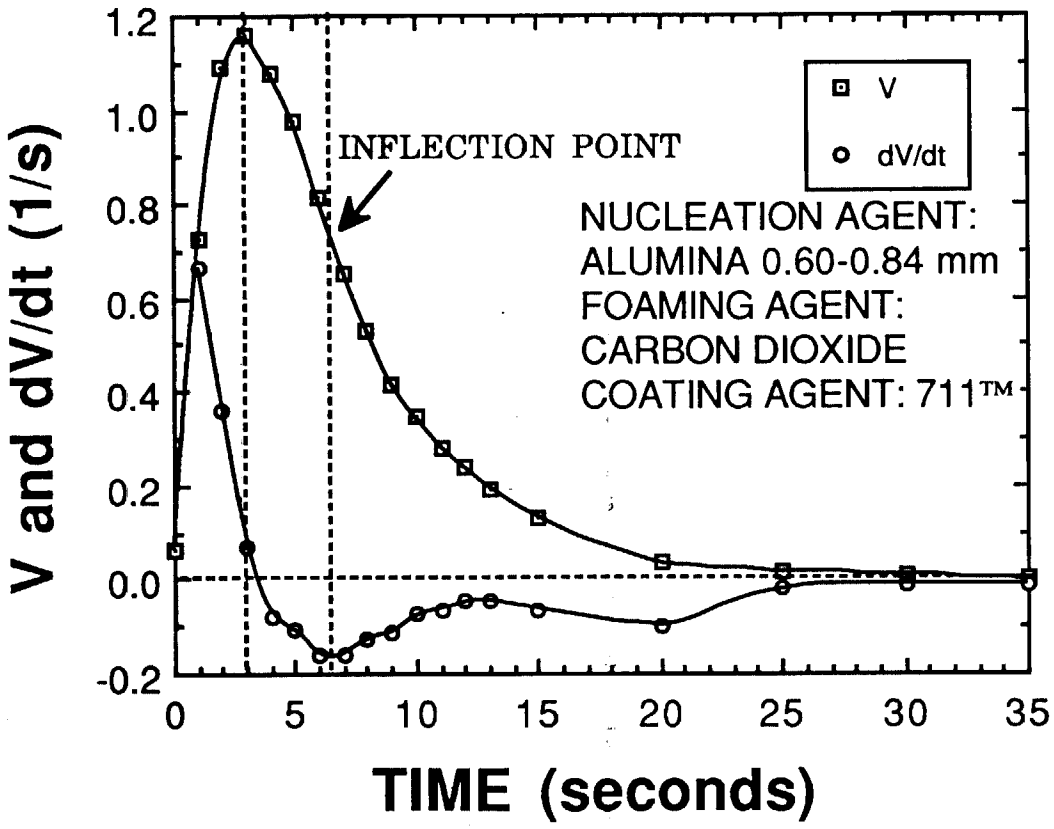

Figure 18: Gas volume and time derivative vs. time for aqueous transient foam with alumina addition.

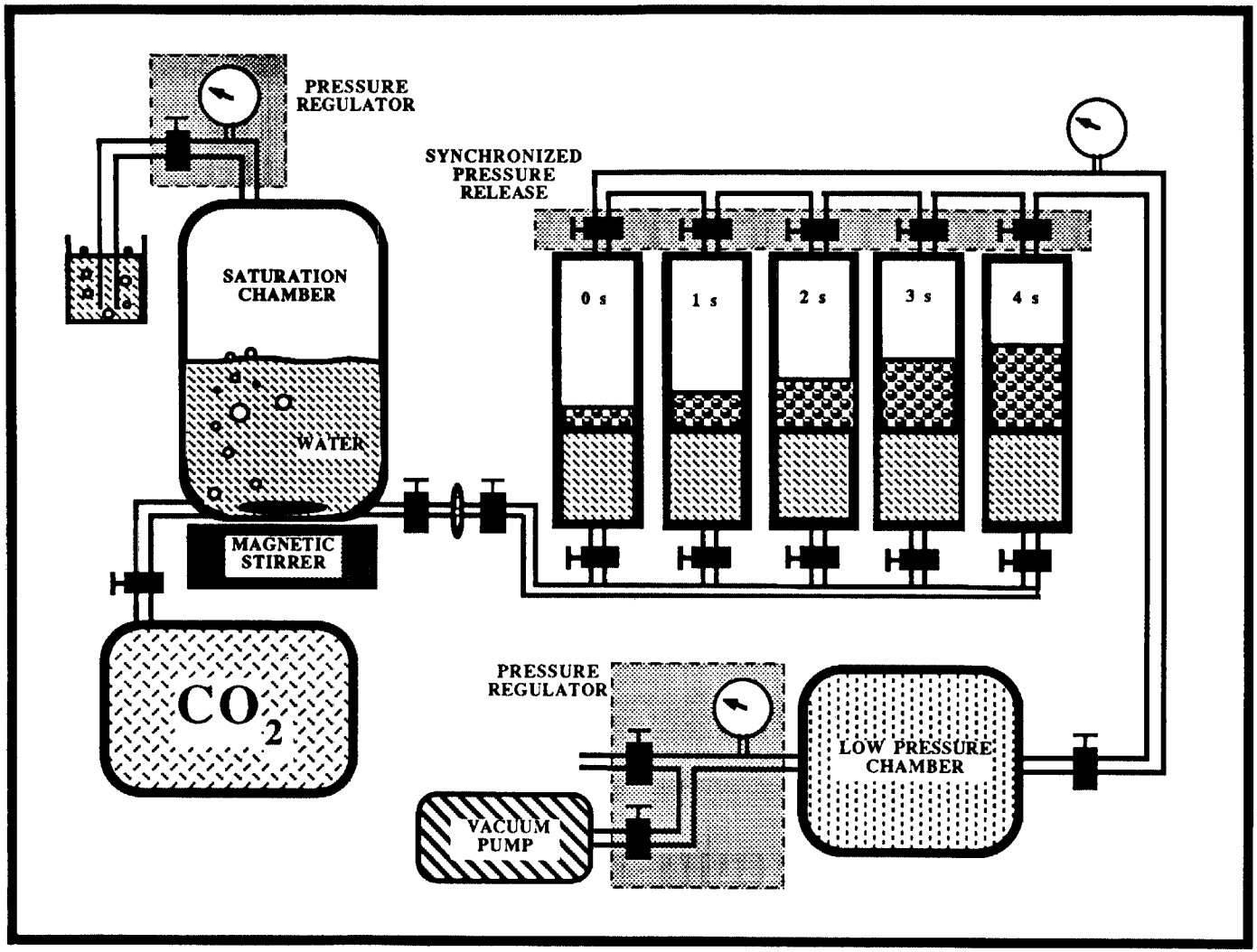

Figure 19: Drop tower experimental set-up for pressure decrease method.

NASA
National Aeronautics and Space Administration

Report Documentation Page

1. Report No.	2. Government Accession No.	3. Recipient's Catalog No.
NASA CR-185208		

4. Title and Subtitle	5. Report Date
Instantaneously Generated Foam and Its Applicability to Reduced Gravity	February 1990
	6. Performing Organization Code

7. Author(s)	8. Performing Organization Report No.
Ali Ilhan, Dong-Sang Kim, and Pavel Hrma	None (E-5282)
	10. Work Unit No. 674-26-05

9. Performing Organization Name and Address	11. Contract or Grant No.
Case Western Reserve University Department of Material Science and Engineering Cleveland, Ohio 44106	NAG3-740
	13. Type of Report and Period Covered Contractor Report Final

12. Sponsoring Agency Name and Address	14. Sponsoring Agency Code
National Aeronautics and Space Administration Lewis Research Center Cleveland, Ohio 44135-3191	

15. Supplementary Notes

Project Manager, Martha H. Jaskowiak, Materials Division, NASA Lewis Research Center.

16. Abstract

The objective of this study is two-fold: (i) understanding the generation and collapse of foam in molten glass and (ii) determining the role of gravity in transient foam dynamics. Both theoretical considerations and experiments show that gravity affects evolution of transient foams. Provided that Marangoni forces are absent, the lack of bubble motion under microgravity will prevent formation of surface foam and, as a result, only bulk foam will be generated. Also, the absence of gravity drainage will affect the foam collapse rate and mode when a surface foam has been produced prior to its exposure to microgravity. The progress of this work follows three steps: (i) selection of appropriate materials and development of experimental techniques, (ii) experimental study of transient foams on earth and developing a theoretical model, and (iii) experimental study of transient foams under microgravity during free fall in a drop tower. This report presents the main results of the first phase of the research which involves most of the ground based work needed to accomplish the first two steps. The suggestions for the final stage of the work is also included. Earth bound experiments have shown that it is possible to produce transient foams suitable for drop tower experiments and to record their behavior by a video or still camera in a simple experimental set-up. Transient cellular foams were produced and studied in soda lime glass with sulfate at 1400-1500 °C. The study of foams in model systems under convenient ambient temperature conditions helped to gather a significant amount of information in a short time. The relationship between foam behavior and structure has been analyzed and the relationship between foam structure and the system properties is currently under development.

17. Key Words (Suggested by Author(s))	18. Distribution Statement
Microgravity Foaming Glass	Unclassified – Unlimited Subject Category 29

19. Security Classif. (of this report)	20. Security Classif. (of this page)	21. No. of pages	22. Price*
Unclassified	Unclassified	58	A04

NASA FORM 1626 OCT 86

*For sale by the National Technical Information Service, Springfield, Virginia 22161

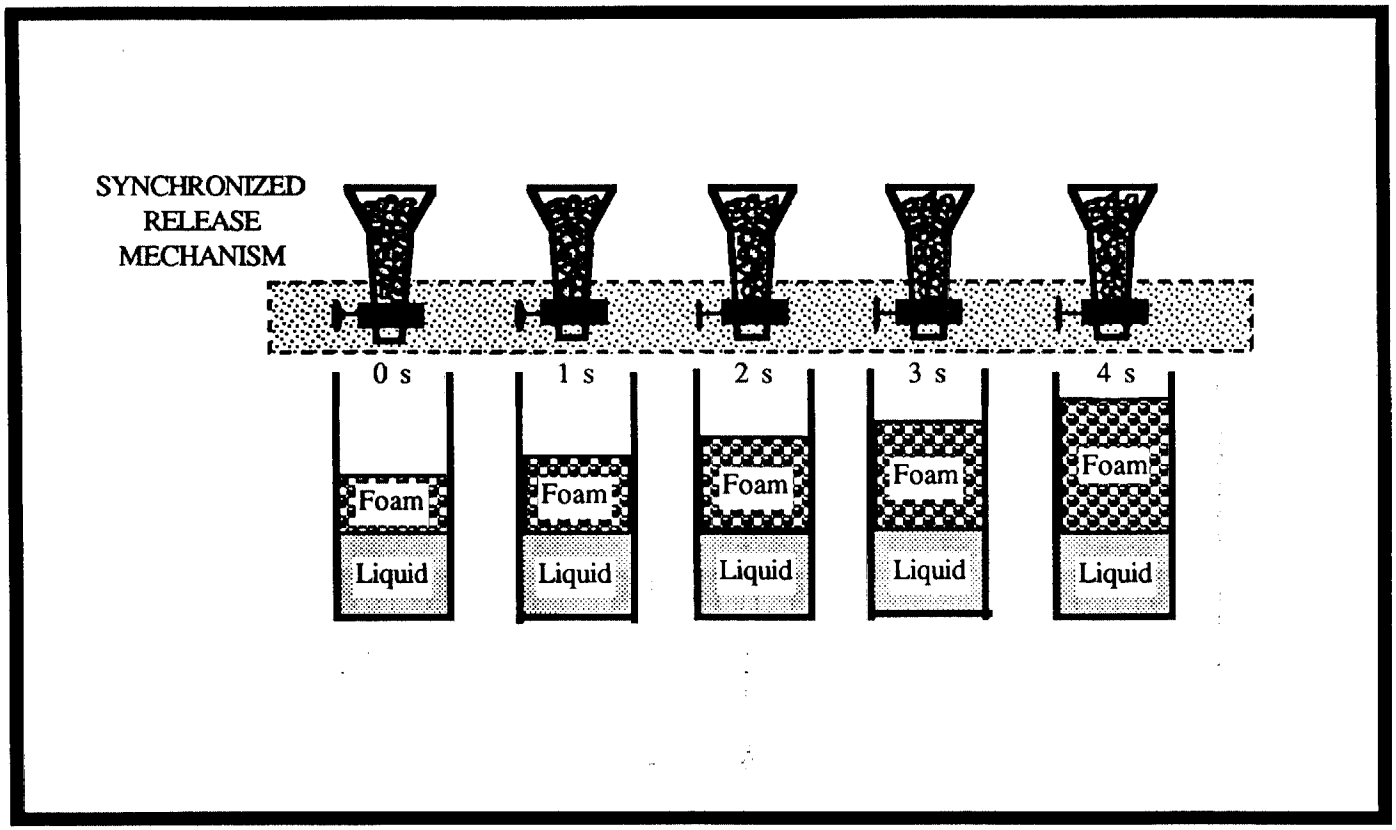

Figure 20: Drop tower experimental set-up for nucleation agent addition method.